A Novel Silver-Containing Antimicrobial potentiates aminoglycoside activity against *Pseudomonas aeruginosa.*

Gracious Yoofi Donkor[a], Greg M. Anderson[a], Michael Stadler[a], Patrick Ofori Tawiah[a], Carl D. Orellano[a], Kevin A. Edwards[b] and Jan-Ulrik Dahl[a#]

[a]School of Biological Sciences, Illinois State University, Microbiology, Normal, IL, USA
[b]School of Biological Sciences, Illinois State University, Cell Biology, Normal, IL, USA

RUNNING TITLE: Reactive oxygen species in antimicrobial therapy

[#]Address correspondence to Jan-Ulrik Dahl, email: jdahl1@ilstu.edu, phone: +1-(309)-438-7694

Word count:
Abstract: 244
Importance: 130
Manuscript: 7158

ABSTRACT

The rapid dissemination of antibiotic resistance combined with the decline in the discovery of novel antibiotics represents a major challenge for infectious disease control that can only be mitigated by investments into novel treatment strategies. Alternative antimicrobials, including silver, have regained interest due to their diverse mechanisms of inhibiting microbial growth. One such example is AGXX®, a broad-spectrum silver containing antimicrobial that produces highly cytotoxic reactive oxygen species (ROS) to inflict extensive macromolecular damage. Due to connections identified between ROS production and antibiotic lethality, we hypothesized that AGXX® could potentially increase the activity of conventional antibiotics. Using the gram-negative pathogen *Pseudomonas aeruginosa*, we screened possible synergistic effects of AGXX® on several antibiotic classes. We found that the combination of AGXX® and aminoglycosides tested at sublethal concentrations led to a rapid exponential decrease in bacterial survival and restored sensitivity of a kanamycin-resistant strain. ROS production contributes significantly to the bactericidal effects of AGXX®/aminoglycoside treatments, which is dependent on oxygen availability and can be reduced by the addition of ROS scavengers. Additionally, *P. aeruginosa* strains deficient in ROS detoxifying/repair genes were more susceptible to AGXX®/aminoglycoside treatment. We further demonstrate that this synergistic interaction was associated with significant increase in outer and inner membrane permeability, resulting in increased antibiotic influx. Our study also revealed that AGXX®/aminoglycoside-mediated killing requires an active proton motive force across the bacterial membrane. Overall, our findings provide an understanding of cellular targets that could be inhibited to increase the activity of conventional antimicrobials.

IMPORTANCE

The emergence of drug-resistant bacteria coupled with the decline in antibiotic development highlights the need for novel alternatives. Thus, new strategies aimed at repurposing conventional antibiotics have gained significant interest. The necessity of these interventions is evident especially in gram-negative pathogens as they are particularly difficult to treat due to their outer membrane. This study highlights the effectiveness of the silver containing antimicrobial AGXX® in potentiating aminoglycoside

activities against *P. aeruginosa*. The combination of AGXX® and aminoglycosides not only reduces bacterial survival rapidly but also significantly re-sensitizes aminoglycoside-resistant *P. aeruginosa* strains. In combination with gentamicin, AGXX® induces increased endogenous oxidative stress, membrane damage and iron sulfur cluster disruption. These findings emphasize AGXX®'s potential as a route of antibiotic adjuvant development and shed light into potential targets to enhance aminoglycoside activity.

INTRODUCTION

The spread of antibiotic resistance has now reached a large number of bacterial pathogens and evolved into a pertinent global health challenge (*1*). Over the past decade, resistance has been reported against all classical antibiotics, including last resort treatments such as polymyxins (*2*). The resistance crisis is further exacerbated in gram-negative pathogens due to the low permeability of their outer membrane and the extensive arsenal of drug resistance mechanisms that these critters employ. One example of a difficult to treat gram-negative bacterium is the opportunistic pathogen *P. aeruginosa*, a common cause of acute (e.g., wounds, burns) and chronic infections (e.g., diabetic ulcers, cystic fibrosis) (*3*). *P. aeruginosa* is characterized by its high intrinsic and acquired resistance mechanisms, allowing the pathogen to thrive in the presence of a large number of antibiotics (*4*).

In light of these challenges, recent studies have focused on alternative treatment strategies to limit bacterial infection and colonization (*5*, *6*). Transition metals, such as silver and copper, have long been recognized for their antimicrobial activities and were already used by the ancient Greeks for would healing (*7*). Despite its long-standing history and high efficiency against bacteria, the antimicrobial mode of action of silver is poorly understood. Pleiotropic effects have been described and include changes in DNA condensation, membrane alteration and protein damage (*7*, *8*). Silver ions have a particularly high affinity for cysteine thiols, disrupt exposed iron-sulfur clusters of dehydratase enzymes, and replace metal-containing cofactors, thus affecting a wide range of cytoplasmic and membrane proteins (*9*, *10*). More recently, silver derivates have

92 received increased attention in medical applications, e.g. as antimicrobial surface-
93 coatings on catheters and implants to protect against biofilm-forming bacteria and to
94 reduce the risk of nosocomial infections (*5*, *11*). One such promising silver-based
95 antimicrobial with broad-spectrum activity is AGXX®. AGXX® consists of micro-galvanic
96 elements of silver (Ag) and ruthenium (Ru), which are surface conditioned with ascorbic
97 acid (*12*, *13*). AGXX® has been used in the form of a powder and implemented as an
98 electroporated sheet on a variety of surfaces, including steel meshes, ceramics and water
99 pipes, to limit bacterial colonization. AGXX®'s antimicrobial is not entirely dependent on
100 the release of silver ions; instead it is proposed to generate reactive oxygen species
101 (ROS), such as hydroxyl radicals (•OH) and superoxide (O_2^-) through a series of redox
102 reactions where the oxidized Ag component is reduced by organic matter and donates
103 electrons to the valent Ru, which subsequently generates O_2^- and other ROS (*12*–*16*).
104 Previous studies revealed that, compared to classical silver and other metals, AGXX®
105 was significantly more bactericidal against gram-positive bacteria such as
106 *Staphylococcus aureus* and *Enterococcus faecalis* (*12*, *13*). Surprisingly, the antimicrobial
107 effects of AGXX® on gram-negative pathogens remain largely unexplored.
108
109 Compounds that generate ROS and/or stimulate endogenous oxidative stress in bacteria
110 have gained interest as potential antibiotic adjuvants (*17*). Adjuvants increase the efficacy
111 of antibiotics by targeting metabolic processes or cellular networks that ultimately lead to
112 a synergistic increase in antibiotic potency (*18*). A classic example for the synergy
113 between adjuvants and antibiotic is the combination of amoxicillin, a beta-lactam
114 antibiotic, and clavulanic acid. Due to clavulanic acid's high affinity for beta-lactamase
115 enzymes, its combination with the beta-lactam antibiotics, such as amoxicillin,
116 synergistically potentiate their activity against penicillin-resistant bacteria (*19*). The
117 hypothesis behind the synergistic effects of ROS-generating or -inducing compounds is
118 based on the multimodal action of these compounds, which could potentially disrupt
119 bacterial targets necessary for the defense of antibiotics (*20*). Recent studies on the
120 bactericidal mode of action of aminoglycoside, fluoroquinolone and beta-lactam
121 antibiotics have also proposed increased endogenous ROS stress as an additional
122 mechanism for bacterial killing (*5*, *20*, *21*). Notably, activation of the bacterial envelope

stress response, hyperactivation of the electron transport chain, and damage of iron sulfur clusters have been shown to contribute to an increase in endogenous ROS level (*5*). Although these findings are controversial, extensive evidence has been presented for the integral role of ROS-mediated damage in antibiotic-induced cell death (*6*). More importantly, recent studies employing ROS-generating compounds have reported promising results on their potential in sensitizing a wide variety of multidrug-resistant bacteria to both bactericidal and bacteriostatic antibiotics (*5*).

Given that AGXX®'s proposed mode of action involves ROS production and studies with focus on evaluating potential synergistic effects of AGXX® on conventional antibiotics are lacking, we started to investigate possible potentiating effects of AGXX® on members of several antibiotic classes, using the *P. aeruginosa* strain PA14 as a model. Exploring potential synergies between AGXX® and antibiotics could provide viable answers to the antimicrobial discovery drought for instance by reducing the minimal inhibitory concentrations of conventional antibiotics required for treatment or possibly overriding and/or delaying antibiotic resistance development (*22*). By exposing PA14 to sublethal concentrations of AGXX® and the antibiotics of interest alone and in combination, we found that bacterial survival was exponentially reduced when the cells were exposed to combinations of AGXX® and aminoglycoside antibiotics. Moreover, combined treatment of both compounds re-sensitized a kanamycin resistant PA14 strain to sublethal concentrations of the antibiotic. We further demonstrate that the combined treatment of AGXX® and aminoglycosides resulted in increased endogenous oxidative stress and a subsequent disruption of iron homeostasis, potentially providing an explanation for the elevated ROS level. The synergy was associated with a significant increase in outer and inner membrane permeability, which facilitates antibiotic influx. Moreover, our studies revealed that the synergy between AGXX® and aminoglycosides relies on an active proton motive force across the bacterial membrane.

RESULTS

AGXX® is more efficient in killing P. aeruginosa than silverdene and silver nitrate. Studies with silver ions suggest that gram-negative bacteria are more susceptible than

154 gram-positive bacteria (*23*). In this study, we investigated the effect of AGXX® on *P.*
155 *aeruginosa* using PA14 as model strain. To compare the effective antimicrobial
156 concentrations of different AGXX® formulations against PA14, we first performed survival
157 analyses in the presence and absence of AGXX383®, AGXX394®, AGXX823®, and
158 AGXX720C®, respectively. While these AGXX® formulations all consist of the galvanized
159 silver/ruthenium complex, they differ in various aspects such as silver ratio, particle size,
160 and production procedure, which may affect their antimicrobial activity. Our time killing
161 assays revealed that AGXX383® and AGXX394® have comparable antimicrobial
162 activities against PA14 and are considerably more potent in inhibiting PA14 growth and
163 survival compared to AGXX823® and AGXX720C® (**Supplementary FIG S1**). Silver
164 derivates have received increased attention in medical applications, e.g. as antimicrobial
165 surface-coatings on catheters that protect from biofilm-forming bacteria and reduce the
166 risk of nosocomial infections (*24*). Moreover, silver is used in topicals to prevent and/or
167 treat infections in wounds (*25*). One such example is silver sulfadiazine (silverdene), the
168 gold standard for treating and preventing *P. aeruginosa* infections in burn wound patients
169 (*26*). However, silverdene is associated with complications such as allergic reactions to
170 the sulfadiazine moiety emphasizing the need for novel treatment therapies (*26*). To
171 compare the antimicrobial activities of AGXX394®, silver nitrate ($AgNO_3$) and silverdene,
172 we conducted survival studies of PA14 in the presence and absence of 25 μg/ml of each
173 compound. Survival of PA14 was highly compromised when cells were exposed to
174 AGXX394® (**FIG.1**). A direct comparison of the killing efficiencies between AGXX394 and
175 silverdene and silver nitrate after 3 hours of treatment revealed a ~1-log and 2-log higher
176 bactericidal activity for AGXX394®, respectively, potentially making AGXX® an attractive
177 treatment/prevention alternative (**FIG. 1).** AGXX treatment has been shown to elicit
178 oxidative stress responses shock responses and other general stress response regulons
179 (*13*). To confirm ROS production of AGXX394®-treated PA14, we quantified intracellular
180 ROS levels using the redox-sensitive molecular probe dichlorodihydrofluorescein
181 diacetate (H_2DCFDA). H_2DCFDA has been extensively demonstrated to detect various
182 ROS, including peroxides as well as peroxyl- and •OH radicals (*27*). When exposed to
183 ROS, the nonfluorescent fluorescent H_2DCFDA, is oxidized to highly green fluorescent
184 2',7'-dichlorofluorescein (DCF) (*27*). We found that exposure to both sublethal (20 μg/ml)

185 and bactericidal (40 µg/ml) levels of AGXX394® caused a 2.5 and 4-fold increase in
186 endogenous ROS levels **(Supplementary FIG S2A)**. Pretreating PA14 with thiourea, an
187 ROS scavenger, resulted in reduced ROS levels and recovered survival at bactericidal
188 AGXX394® concentrations (40 µg/ml) **(Supplementary FIG S2A&B)**.
189
190 ***AGXX® exponentially increases the activity of aminoglycosides against P.***
191 ***aeruginosa.*** Our next goal was to determine how the presence of AGXX would affect
192 antibiotic activity against *P. aeruginosa.* Specifically, we were interested in determining
193 whether combining AGXX® with members of different antibiotic classes, such as
194 inhibitors of DNA replication (fluoroquinolones), cell wall biosynthesis (β-lactams), folate
195 biosynthesis, membrane integrity (polymyxins), and translation (aminoglycosides), show
196 increased bactericidal activity against *P. aeruginosa*. Here, we used AGXX720C®, a
197 formulation with significantly lower antimicrobial activity that allowed us to control dosage
198 of AGXX® more reliably (**Supplementary FIG S1**). We determined the minimal inhibitory
199 concentrations (MIC) of AGXX720C® and ten members of five different antibiotic classes
200 in PA14, which were cultivated under aerobic conditions in Mueller-Hinton broth
201 (**Supplementary Table S1**). Using time killing assays, we exposed PA14 to sublethal
202 concentrations of AGXX720C® (75 µg/ml), the indicated antibiotics, and their
203 combinations at the same sublethal concentrations that were used for the individual
204 treatments, respectively. We monitored colony forming units counts every 60 min over a
205 time course of three hours (**FIG 2; Supplementary FIG S3**) and calculated the percent
206 survival for each sample at the 3-hour time point relative to the untreated control (**FIG 2)**.
207 None of the individual treatments with either 75 µg/ml AGXX720C® or any of the
208 antibiotics resulted in substantial killing of PA14 (**FIG 2; Supplementary FIG S3**). The
209 combination of 75 µg/ml AGXX720C® with 35 ng/ml ciprofloxacin and 100 ng/ml
210 norfloxacin, respectively, resulted in PA14 survival comparable to the individual
211 treatments suggesting that AGXX® does not potentiate the bactericidal activities of
212 fluoroquinolones against PA14 (**FIG 2A; Supplementary FIG S3A, B**). Likewise, the
213 combined treatments of AGXX720C® and 78 µg/ml carbenicillin, 0.156 µg/ml imipenem,
214 or 125 µg/ml trimethoprim did not significantly change PA14 survival compared to their
215 individual treatments (**FIG 2B, C; Supplementary FIG S3C**). On the other hand, we found

216 that the bactericidal activity of the membrane targeting antibiotic polymyxin B was
217 increased by the presence of AGXX720C® as evidenced by a 1-log reduction in PA14
218 survival as compared to AGXX720C® or polymyxin B alone, which each caused less than
219 5% killing (**FIG 2D; Supplementary FIG S3D**). However, we observed the most drastic
220 decrease in PA14 survival when AGXX720C® was combined with a member of
221 aminoglycoside antibiotics, even at concentrations far below the MIC. Co-treatment of
222 AGXX720C® with 0.4 µg/ml gentamicin (Gm) (0.2x MIC) reduced PA14 survival by as
223 much as 4 logs after three hours of treatment (**FIG 2E; Supplementary FIG S3E**), while
224 combinations of AGXX720C® with 2 µg/ml amikacin (0.27x MIC), 1 µg/ml tobramycin
225 (0.4x MIC), or 3 µg/ml streptomycin (0.15x MIC) caused up to 3 log reduction in survival
226 (**FIG 2E, Supplementary FIG S3F-H**).
227 It has been reported that $AgNO_3$'s synergizing effects on aminoglycosides was reduced
228 in minimal media (*28*). We therefore exposed PA14 sub-cultured in MOPS-glucose
229 (MOPSg) minimal medium to increasing sublethal AGXX concentrations alone or in
230 combination with a sublethal gentamicin **(Supplementary FIG S4A)**. Increasing AGXX®
231 concentrations significantly reduced PA14 survival in a dose-response like manner
232 **(Supplementary FIG S4A)**. Considering that casamino acid (CAS) supplementation was
233 also reported to partially restore $AgNO_3$'s effects in minimal media, we replicated our time
234 killing assays in MOPSg media in the presence of 0.2% CAS. Surprisingly, addition of
235 0.2% CAS decreased AGXX®'s effects on Gm in MOPSg medium **(Supplementary FIG**
236 **S4B)**. Although, we do not probe the reasons behind the effects of casamino acids in
237 minimal media, it is evident that AGXX® synergizes with aminoglycosides in both rich and
238 minimal media.
239
240 ***AGXX® increases the sensitivity of P. aeruginosa strain PA14 to kanamycin.***
241 Considering the significant increase in lethality upon concurrent exposure of PA14 to
242 AGXX720C® and aminoglycosides, we sought to determine whether the addition of
243 AGXX720C® could reintroduce sensitivity in aminoglycoside-resistant *P. aeruginosa*
244 strains. Like many other *P. aeruginosa* strains, PA14 is intrinsically resistant to many
245 different antibiotics, including the aminoglycoside kanamycin. Under the conditions
246 tested, our PA14 strain showed a MIC of 240 µg/ml for kanamycin. We then exposed

247 PA14 to 75 µg/ml AGXX720C®, 50 µg/ml kanamycin, or a combination of 75 µg/ml
248 AGXX720C® and 50 µg/ml kanamycin and determined their survival over the time course
249 of 3 hours as described before. As early as 60 minutes post treatment, the combination
250 of AGXX720C® and kanamycin reduced colony survival by ~1.5 log, which increased to
251 about 4 log (10,000-fold) difference in survival after 3 hours (**FIG 3**). In summary, we
252 conclude from our data that AGXX® potentiates the activity of a wide range of
253 aminoglycoside antibiotics, potentially making aminoglycoside-resistant *P. aeruginosa*
254 strains more sensitive again.
255
256 ***The combination of sublethal concentrations of AGXX® and aminoglycosides***
257 ***increases ROS formation and causes upregulation of genes indicative of DNA***
258 ***damage and protein aggregation.*** AGXX®'s main antimicrobial mode of action is
259 mediated by the generation of ROS (39). Increased endogenous oxidative stress has also
260 been linked to the lethality of aminoglycosides and other bactericidal antibiotics (*29*, *30*).
261 It may therefore be possible that a disruption in the redox balance during antibiotic
262 exposure increases lethality by amplifying the adventitious generation of ROS by
263 antibiotics. We treated exponentially growing PA14 for 60 min with sublethal
264 concentrations of Gm (0.25 µg/ml), AGXX720C® (50 µg/ml), or their combination and
265 compared H2DCFDA fluorescence in each sample to the untreated control. Individual
266 treatments with either Gm or AGXX720C® did not result in a significant increase in
267 H_2DCFDA fluorescence, excluding the possibility that substantial amounts of ROS were
268 formed at these sublethal concentrations (**FIG 4A**). However, when applied in
269 combination, we observed an 8-fold increase in H_2DCFDA fluorescence indicative of
270 increased ROS production under these conditions. Pre-treatment of PA14 with the ROS
271 scavenger thiourea (*31*) or the hydrogen peroxide (H_2O_2) -detoxifying enzyme catalase
272 resulted in a significant decline in H_2DCFDA fluorescence (**FIG 4A**) as well as restored
273 PA14 survival by 2- to 4-log, respectively (**FIG 4B; Supplementary FIG S5A**). Thus, our
274 data suggest that the high antimicrobial activity of the combinational treatment can at least
275 in parts be explained by increased ROS formation. However, H_2DCFDA is rather
276 unspecific and detects numerous ROS compounds. We therefore followed up on our
277 observation with the use of additional, more specific ROS-detecting fluorescent dyes. We

278 used the boronate-based peroxy orange 1 (PO1) dye as well as hydroxyphenyl
279 fluorescein (HPF) to examine intracellular concentrations of H_2O_2 and •OH levels,
280 respectively (*32*, *33*). After 1 hour of treatment, we detected a significant shift in PO1 and
281 HPF fluorescence, indicating that both H_2O_2 and •OH are produced in AGXX720C®/Gm-
282 treated PA14 (**FIG 4C, D; Supplementary FIG S5B, C**).
283
284 To deal with the negative consequences of ROS and eliminate ROS-mediated damage,
285 microorganisms have evolved intricate systems to maintain and restore a balanced redox
286 homeostasis and repair ROS-mediated damage [recently reviewed in (*34–39*)]. Proteins
287 and nucleic acids represent the most prevalent targets of ROS (*40*, *41*). To test whether
288 the elevated ROS production causes macromolecular damage, we analyzed the
289 transcript level of *ibpA* and *sulA,* two genes that have previously been shown to be
290 upregulated when cells experience severe oxidative stress (*42*, *43*), in PA14 cells treated
291 with Gm and AGXX alone and in combination. *ibpA* encodes a molecular chaperone,
292 which plays a significant role in protecting bacteria from proteotoxic stressors including
293 ROS (*44*). *sulA* encodes the cell division inhibitor SulA, which is part of the SOS response
294 and induced when the cell experiences DNA damage, a possible consequence of
295 oxidative stress (*45*). We exposed exponentially growing PA14 cells to sublethal
296 concentrations of AGXX720C®, Gm, or the combination thereof for 60 min and quantified
297 *ibpA/sulA* mRNA level. While individual treatments with sublethal concentrations of
298 AGXX720C® or Gm did not cause significant changes in *ibpA/sulA* expression, their
299 transcript levels were approximately 5-fold (*sulA*) and 100-fold (*ibpA*) increased when
300 PA14 was treated with the combination of AGXX720C® and gentamicin, indicating
301 significant macromolecular damage **(FIG 4E)**.
302
303 ***Anaerobic growth and antioxidant systems provide protection against ROS-***
304 ***mediated damage caused by a combinational treatment of AGXX® and***
305 ***aminoglycosides****.* To provide additional evidence that ROS contribute to the synergy
306 between aminoglycosides and AGXX®, we determined whether their killing efficiency
307 depends on the presence of molecular oxygen, which is essential for ROS production.
308 PA14 was grown in MHB under either aerobic or anaerobic conditions and treated with

309 sublethal concentrations of gentamicin, AGXX720C® or the combination thereof. When
310 grown anaerobically, MHB was supplemented with 1% KNO_3 to stimulate the proton
311 motive force (PMF). Anaerobically respiring PA14 cells tolerated treatments with AGXX®
312 and 0.5 µg/ml Gm (0.25x MIC) fairly well and showed about 2.5 log higher survival relative
313 to aerobically grown cells exposed to the same treatment. However, when we increased
314 the Gm concentration to 1 µg/ml (0.5x MIC) in the in the presence of AGXX®, PA14
315 survival also declined albeit at a lower rate than aerobically growing cells under the same
316 conditions **(FIG. 5A)**.
317 Next, we tested the susceptibility of PA14 strains with transposon insertions in genes that
318 have previously been identified as major oxidative stress response and/or defense
319 systems. We exposed PA14 transposon mutant strains (*46*) with defects in *oxyR*
320 (encodes ROS-sensing transcriptional regulator OxyR), *katA* (encodes catalase KatA),
321 *katB* (encodes catalase KatB), and *dps* (encodes an iron acquisition protein in response
322 to oxidative stress) to sublethal concentrations of AGXX720C® (25 µg/ml), tobramycin
323 (0.25 µg/ml), or the combination thereof for 3 hours and compared their colony survival
324 to that of the corresponding wildtype strain PA14 (**FIG. 5B**). We found that strains deficient
325 in functional copies of *katA* and *dps* showed a little over 1 log reduced survival compared
326 to wildtype cells, while no difference in survival was observed for cells lacking the
327 hydrogen peroxide global regulator OxyR and catalase KatB, respectively (**FIG. 5B**).
328 Taken together, our findings point towards a relevant role for ROS generation in the
329 synergistic interaction between aminoglycosides and AGXX®.
330
331 ***The synergy between AGXX® and aminoglycosides on PA14 killing is in parts***
332 ***mediated by a disruption in iron homeostasis.*** Fe/S cluster are essential cofactors in
333 various metabolic enzymes, including members of the electron transport chain and the
334 tricarboxylic acid cycle (TCA) cycle (*47*). Fe/S cluster are particularly vulnerable to ROS,
335 which negatively impacts the activity of metabolic enzymes and ultimately cellular
336 metabolism during oxidative stress. Likewise, silver has been found to disrupt Fe/S
337 clusters in proteins (*10*), resulting in a cellular increase in free iron, which in turn can
338 stimulate •OH formation via Fenton reaction and cause extensive macromolecular
339 damage (*7*). Moreover, Fe/S disruption and Fenton-mediated •OH production have been

340 proposed as a downstream consequences of aminoglycoside killing (*30*). Given the
341 elevated •OH level (**FIG 4D; Supplementary FIG S5C**) and increased susceptibility of a
342 *dps*-deficient strain upon PA14 exposure to the AGXX®/Gm combination (**FIG 5B**), we
343 wondered whether the increased ROS production impairs the activity of Fe/S cluster-
344 containing enzymes. We prepared cell lysates from PA14 exposed to individual or
345 combined AGXX® and Gm, and measured the activity of aconitase, an Fe/S-containing
346 enzyme of the TCA cycle, whose activity depends on the presence of the Fe/S-cluster.
347 While individual treatments with sublethal AGXX720C® or Gm concentrations had no
348 impact on aconitase activity, exposure to a combination of AGXX720C® and Gm resulted
349 in ~75% loss in activity (**FIG 6A**). The loss in aconitase activity could be explained by the
350 release of iron atoms, as it occurs during Fe/S cluster oxidation under $O_2^-$and H_2O_2 stress
351 (*47*, *48*). To test the role of free iron for the synergistic effect between AGXX720C® and
352 aminoglycosides, we treated PA14 with the iron chelator 2',2' bipyridyl prior to their
353 exposure to sublethal concentrations of AGXX720C® and Gm. Indeed, we found that
354 PA14 survival was less impaired when cells had been treated with 2',2' bipyridyl prior to
355 the presence of the AGXX720C®/Gm cocktail **(FIG 6B)**. However, iron chelators, such as
356 2',2' bipyridyl, have been reported to reduce aminoglycoside killing in *E. coli,* a
357 phenomenon we confirmed in *P. aeruginosa* **(Supplementary FIG S5D)**. Overall, our
358 data suggest a potential role of free iron for the ROS-mediated toxicity of aminoglycoside
359 exposure when in synergy with AGXX®.
360
361 ***Combined AGXX® and aminoglycoside treatment induces significant membrane***
362 ***damage.*** In the initial stages of aminoglycoside uptake, the polycationic aminoglycoside
363 electrostatically interacts with the bacterial outer membrane, displacing membrane
364 divalent cations and inevitably increasing membrane permeability (*49*). Thus, compounds
365 with membrane permeabilizing properties have been reported as potent aminoglycoside
366 adjuvants (*50*, *51*). To probe the role of membrane permeability, we evaluated outer
367 membrane disruption using the hydrophobic fluorescent probe N-phenyl-1-napthylamine
368 (NPN), which has diminished fluorescence in the presence of an intact outer membrane
369 but significantly increases when bound to exposed phospholipid groups in a disrupted
370 lipopolysaccharide monolayer (*52*). We found that in contrast to individual treatments with

371 sublethal AGXX720C® and Gm concentrations, a combined treatment significantly
372 increased NPN uptake, resulting in ~7-fold higher NPN fluorescence (**FIG 7A**). Next, we
373 examined the inner membrane permeability of PA14 cells that were subjected to
374 AGXX720C® and Gm treatment alone and in combination, using the fluorescent probe
375 propidium iodide (PI). Due to its size and charge, PI can only cross compromised inner
376 membranes where it binds nonspecifically to nucleic acids enhancing its fluorescence
377 exponentially (*53*). Individual treatments with sublethal AGXX720C® and gentamicin
378 concentrations did not result in significantly increased PI fluorescence (**FIG 7B**)
379 suggesting that at these concentrations none of them causes significant plasma
380 membrane damage. A combined treatment, however, led to substantially increased PI
381 fluorescence. Our spectrophotometric findings were complemented by fluorescent
382 microscopy analyses of PA14 cells that were treated as described before, washed in PBS,
383 stained with Syto9/PI (live/dead stain), incubated in the dark for 15 minutes at room
384 temperature, mounted onto a glass slide with 1% agarose, and imaged at 63x
385 magnification via inverted confocal microscopy. While the individual treatments with 0.25
386 µg/ml Gm or 50 µg/ml AGXX720C® only caused increased PI fluorescence in very few
387 cells, the number of PI-stained cells was substantially higher in PA14 cells that were
388 treated with a combination of sublethal AGXX720C®/Gm concentrations (**FIG 7C**).
389
390 ***AGXX® increases aminoglycoside uptake and lethality through increased activity***
391 ***of the proton motive force (PMF).*** Considering the significance of membrane
392 permeability for aminoglycoside uptake, we reasoned that the increased membrane
393 disruption PA14 experiences during a combined treatment of AGXX® and
394 aminoglycosides would facilitate intracellular accumulation of aminoglycosides. Using
395 flow cytometry, we evaluated the uptake of Texas-Red-labelled Gentamicin (TR-Gm) in
396 exponentially growing PA14 in the presence or absence of AGXX720C®. Treatment of
397 PA14 with a combination of AGXX720C® and TR-Gm resulted in a significant increase in
398 TR-Gm uptake similar to treatments with the membrane-targeting antibiotic polymyxin B
399 (**FIG 8A, Supplementary FIG S6A).** The increased uptake of TR-Gm in the presence of
400 AGXX® resulted in a 2.5 log reduction in bacterial survival compared to PA14 that were
401 only exposed to TR-Gm alone **(Supplementary FIG S6B**). Moreover, the secondary and

402 tertiary stage of aminoglycoside import appears to depend on an active membrane
403 potential and occurs therefore only in actively respiring cells (*49*, *54*). As such, increasing
404 cellular respiration or stimulation of membrane potential has been found to increase
405 aminoglycoside lethality (*55*). Using the protonophore CCCP, a compound that efficiently
406 inhibits the proton motive force (PMF), we determined whether the synergy between
407 AGXX® and aminoglycosides is dependent on the membrane potential. Not surprisingly,
408 PA14 killing by a lethal dose of gentamicin (1 µg/ml) could be reduced by almost 2 logs
409 when the cells were pre-incubated with CCCP (**Supplementary FIG S6C).** Likewise,
410 pretreatment with CCCP restored PA14 survival to a similar degree in the presence of
411 0.25 µg/ml Gm and 50 µg/ml AGXX720C® for three hours **(Fig. 8B).** Surprisingly,
412 combining polymyxin B at 1x MIC and 2x MIC with sublethal Gm concentrations did not
413 result in increased killing relative to polymyxin B alone **(Fig. S2D)**. Overall, our findings
414 indicate that AGXX®'s synergistic effect on aminoglycoside lethality does not only involve
415 increased membrane permeability but also requires an active proton motive force across
416 the bacterial membrane.
417

418 **DISCUSSION**

419 In the present study, we demonstrate evidence that the novel silver containing
420 antimicrobial AGXX® may potentially be used an antibiotic adjuvant with activity on the
421 opportunistic pathogen *P. aeruginosa*. We show that AGXX® serves as an efficient tool
422 to potentiate the activity of aminoglycoside antibiotics by reducing bacterial survival up to
423 50,000-fold. Aside from a 1-log increase in killing found when the Ag/Ru complex was
424 combined with the membrane-targeting antibiotic polymyxin B, AGXX® did not influence
425 the activity of antibiotics targeting DNA replication, cell wall synthesis, or folate
426 metabolism **(FIG 2)** raising the possibility that AGXX®'s potentiating effects could be
427 linked to a malfunction in protein synthesis. AGXX®'s potentiating effect was not limited
428 to select aminoglycosides but applied to all members tested, including gentamicin,
429 streptomycin, amikacin, and tobramycin (**FIG 3**). We observed the exponential killing of
430 the AGXX®/aminoglycoside combination in complex and minimal media independent of
431 the presence or absence of amino acids, indicating that the media composition has only
432 minor effects on the synergistic effect (**Supplementary FIG S3)**. Additional support for

433 AGXX®'s stimulating effect on aminoglycoside activity was provided by its ability to re-
434 sensitize a kanamycin resistant *P. aeruginosa* strain (**FIG 4**). Notably, both AGXX® and
435 aminoglycoside antibiotics were present at concentrations far below their MICs (0.1-0.3x
436 MIC) indicating that the combination between the compounds was quite powerful with
437 regards to increasing the bactericidal activity of aminoglycosides.
438
439 Based on our findings, we propose the following model for the synergy between AGXX®
440 and aminoglycoside antibiotics (**FIG 9**): The antimicrobial action of AGXX® is proposed
441 to involve O_2^- and H_2O_2, which are generated in a redox cycle between silver (Ag) and
442 ruthenium (Ru^{x+1}) (*15*, *16*). While the location of AGXX®-mediated ROS production was
443 not the focus of this study, we propose that ROS is mainly generated in the extracellular
444 part before the compounds penetrate the cell. This assumption is based on our finding
445 that exogenous addition of catalase was highly effective in reducing ROS level and
446 increasing *P. aeruginosa* survival upon treatment with a combination of AGXX® and Gm
447 (**Supplementary FIG S5A**), given that catalase cannot readily cross the bacterial cell
448 envelope. The combination of AGXX® and aminoglycosides concertedly increased
449 endogenous ROS levels, including H_2O_2 and •OH. Potentially facilitated by released silver
450 ions, the increased ROS level may disrupt iron-sulfur clusters in metabolic enzymes such
451 as aconitase, resulting in the release of free iron, which ultimately triggers •OH formation
452 in a Fenton reaction (*56*). Increasing ROS levels can inflict macromolecule damage such
453 as DNA damage, protein aggregation, and membrane damage, as evidenced by *(i)* the
454 increased expression of members of the SOS and heat shock responses, and *(ii)* the
455 possibility that the observed damage on outer and inner membrane is mediated by ROS.
456 In either way, increased ROS production contributes to the enhanced killing of *P.*
457 *aeruginosa* upon treatment with a combination of AGXX® and aminoglycosides. The
458 synergistic effect between AGXX® and aminoglycosides is also mediated by an increased
459 uptake and the cellular accumulation of aminoglycosides, which can be attenuated by
460 disrupting the bacterial membrane potential with ionophores such as CCCP.
461
462 The antimicrobial effects of silver and silver containing agents have been extensively
463 documented (*57–59*). However, in spite of the increasing use of silver in antimicrobial

464 applications, its mechanism of action remains to be poorly understood (*24*, *60*, *61*). Silver
465 along with other ROS inducing agents have been proposed to induce an array of
466 multimodal cytotoxic events, including the mis-metalation of proteins, DNA damage, and
467 imbalanced redox homeostasis, which ultimately disrupt multiple bacterial networks
468 leading to cell death (*5*, *17*, *62*). Thus, we investigated whether AGXX®, through its
469 multimodal effects as an ROS inducing compound, could increase that activity of
470 conventional antibiotics against *P. aeruginosa*. AGXX® itself has been proposed to exert
471 its antimicrobial action through the generation of ROS rather than the release of silver
472 ions. AGXX®-mediated ROS production likely starts with the generation of O_2^-, which
473 subsequently can be dismutated by cellular superoxide dismutases into hydrogen
474 peroxide (*15*, *63*). Likewise, aminoglycosides have also been posited to induce metabolic
475 alterations that induce endogenous ROS levels (*64*). Growth of *P. aeruginosa* under
476 anaerobic conditions provided a protective effect against the bactericidal effects of
477 AGXX®/aminoglycoside killing **(FIG 5A)**. Considering that the availability of nitrate as an
478 alternative electron acceptor would facilitate PMF activity during anaerobic growth, a
479 decrease in killing efficiency points towards a relevant role for ROS in the synergistic
480 combination of the two compounds. At higher gentamicin concentrations, however,
481 AGXX® sensitized *P. aeruginosa* to gentamicin **(FIG 6A),** which could be potentially
482 explained with an increase in aminoglycoside uptake due to the high gentamicin
483 availability.
484
485 We found a significant increase in hydrogen peroxide and •OH radical signals upon
486 exposure of PA14 to a combination of AGXX® and aminoglycoside as evidenced by
487 increased PO1 and HPF fluorescence **(FIG 4)** and decreased survival of transposon
488 insertion strains defective in KatA and Dps **(FIG 5B)**. Surprisingly, a transposon insertion
489 into the *oxyR* gene, encoding the major hydrogen response regulator OxyR, did not show
490 a significant difference in survival relative to the wildtype under combined
491 AGXX®/aminoglycoside exposure **(FIG 5B).** However, this is consistent with a previous
492 study on the aminoglycoside potentiating effects of silver nitrate, in which neither *oxyR*-
493 deficient strains nor strains that constitutively express OxyR had significant effects on
494 bacterial survival (*28*). On the other hand, in a different study overexpression of the H_2O_2

495 detoxifying gene, *ahpF,* attenuated the lethality and proteotoxic effects of
496 aminoglycosides, providing evidence for the relevance of oxidative stress in
497 aminoglycoside toxicity (*65*). Previous studies have demonstrated that pretreatment with
498 antioxidant molecules such as thiourea reduced intracellular •OH radical levels and
499 increased bacterial survival during aminoglycoside and silver stress (*17*, *30*, *66*, *67*).
500 Consistent with these findings, we made similar observations as the addition of either
501 catalase or thiourea to AGXX®-aminoglycoside-treated PA14 resulted in a significant
502 reduction in endogenous ROS level as well as bacterial killing relative to the combined
503 treatment alone **(FIG 4A, B; Supplementary FIG S5A, B)**. Consistent with our previous
504 report that AGXX® causes protein aggregation (*68*), we found significant transcriptional
505 upregulation of *ibpA*, which encodes the molecular chaperone IbpA*,* during exposure to
506 AGXX® and Gm. Given that IbpA serves as the front line defense to limit the aggregation
507 of unfolded proteins (*44*), AGXX®/Gm-induced oxidative stress likely causes an
508 imbalance of proteostasis and increases the cellular demand for chaperone expression.
509 Interestingly, heat-shock mediated protein aggregation was found to exponentially
510 increase aminoglycoside lethality in several gram-negative bacteria (*69*). Like our study,
511 this novel mechanism was attenuated under ROS quenching conditions (*69*), providing
512 additional evidence for the relevance of ROS in aminoglycoside killing. Considering that
513 individual AGXX® or gentamicin treatments did not result in a significant increase in ROS
514 signals, it is plausible that applying these antimicrobials at concentrations far below the
515 MIC would not induce the physiological/metabolic alterations necessary for aggravating
516 endogenous ROS levels.
517
518 Considering that both O_2^- and silver ions have been reported to destabilize Fe/S cluster
519 proteins resulting in the release of solvent-exposed iron (*10*, *70*), we investigated the
520 effects of individual and combinational treatments with AGXX® and/or aminoglycoside
521 antibiotics on the activity of aconitase, an Fe-S cluster containing enzyme. We found
522 aconitase to be extremely sensitive towards exposure to both antimicrobials when
523 administered in combination (**FIG 6A**). Disrupted Fe-S clusters could potentially lead to
524 an increase in intracellular iron levels and subsequent •OH generation through Fenton
525 reaction as it has been demonstrated under hydrogen peroxide stress in ROS-sensitive

526 *E. coli* strains (*71*). This would explain the significantly higher •OH levels detected in PA14
527 cells that were exposed to a combined AGXX® and gentamicin mixture **(FIG 4D)**, which
528 could cause significant DNA damage and induce the SOS response. In fact, we found
529 that the combination of sublethal AGXX® and gentamicin significantly induced the
530 expression of *sulA,* an SOS response marker of DNA damage **(FIG 4E)**. Likewise,
531 addition of 2',2' bipyridyl resulted in a 1-log increase in bacterial survival when cells were
532 exposed to the toxic cocktail of gentamicin and AGXX® suggesting that free iron
533 contributes to the bactericidal effects **(FIG 6B)**. However, a similar protective effect was
534 observed in the presence of lethal Gm concentrations, suggesting that the possibility that
535 the rescuing effect in the presence of BIP could be due to its limiting effect on
536 aminoglycoside uptake and not necessarily a quenching of hydroxyl radical generation
537 through Fenton reactions. The Ezraty lab has demonstrated that bipyridyl inhibits Fe-S
538 biosynthesis under iron limiting conditions, resulting in reduced respiratory complex I and
539 II activities and decreased PMF, which is necessary for aminoglycoside uptake (*28*). All
540 in all, our findings highlight the relevance of oxidative stress in the enhancement of
541 antibiotic lethality in *P. aeruginosa* exposed to sub-inhibitory concentrations of AGXX®
542 and aminoglycosides.
543
544 Compared to other gram-negative pathogens, *P. aeruginosa* possesses high intrinsic
545 resistance mechanisms towards a variety of antibiotics (*72*). This resistance is mediated
546 in part by its extensive arsenal of efflux pumps and significantly lower outer membrane
547 permeability (*72*). We found that combining AGXX® and gentamicin increased both inner
548 and outer membrane permeability in *P. aeruginosa* leading to a subsequent increase in
549 aminoglycoside uptake **(FIG 7, FIG 8)**. Aminoglycosides are polycationic in nature and
550 known to displace divalent cations that cross-bridge lipopolysaccharides, which makes
551 the outer membrane substantially more permeable (*73*, *74*). It is therefore possible that
552 AGXX®, much like aminoglycosides, disrupts the outer leaflet of the outer membrane,
553 with the result that lower amounts of aminoglycosides are required to permeabilize *P.*
554 *aeruginosa*. If this were true, we would suspect that the initial stages of aminoglycoside
555 uptake could likely be accelerated causing a more rapid antibiotic influx. Surprisingly, we
556 found that the addition of sublethal polymyxin B concentrations did not affect gentamicin

557 lethality indicating that the mechanism behind the potentiating effects of AGXX® extends
558 beyond increased membrane permeability **(Supplementary FIG S6D)**. We further found
559 that disrupting membrane potential using an ionophore increased bacterial survival under
560 combined AGXX® and gentamicin stress **(FIG 8)**, suggesting an important role for the
561 energy dependent phase of aminoglycoside uptake AGXX®'s potentiating effect, as has
562 been found with strategies that increase aminoglycoside lethality via TCA cycle mediated
563 PMF generation (*55*).
564 By definition, antibiotic adjuvants do not possess inherent antimicrobial activity (*75*). Even
565 though AGXX® can technically not be defined as an antibiotic adjuvant given its own
566 antimicrobial activity (*16*), our use of sublethal AGXX® concentrations to screen for
567 potentiating effects satisfied this definition. Notably, the antimicrobial properties of silver
568 have been accepted for a long time and taken advantage of in topical ointments such as
569 silverdene cremes to prevent and treat *P. aeruginosa* infections in burn wound patients
570 (*26*). A comparison to silver nitrate and silver sulfadiazine (silverdene) revealed an
571 increased potency of some of the AGXX® formulations resulting in a lower survival rate
572 of PA14 **(FIG 1)**. Moreover, given that antibacterial combination therapies typically involve
573 significantly lower concentrations of the antimicrobials compared to what is needed for
574 individual treatments, such approaches would potentially delay resistance development.
575

576 ## MATERIALS AND METHODS

577 **Bacterial strains and growth conditions.** Unless stated otherwise, overnight *P.*
578 *aeruginosa* PA14 strains **(Supp. Table 2)** were grown under aerobic conditions in Luria-
579 Bertani broth (LB, Millipore Sigma) at 37°C for 16-20 hours at 300 rpm. For subsequent
580 assays, overnight cultures were diluted into Mueller-Hinton broth (MHB) or 3-(N-
581 morpholino) propanesulfonic acid minimal media containing 0.2% glucose, 1.32 mM
582 K_2HPO_4 and 10 µM thiamine (MOPSg) and incubated at 37 °C at 150 rpm. Growth under
583 anaerobic conditions was performed as described previously (*76*). In brief, PA14 was
584 grown anaerobically in the presence of 1% KNO_3 in a 50 ml falcon tube that was
585 additionally sealed with parafilm. Growth was performed in DuoClick™ (Thomas
586 Scientific) screw cap culture tubes filled with minimal room. Overnight PA14 cultures were

587 diluted to an OD_{600}=0.002 in MHB containing 1% KNO_3 and grown until OD_{600} ~0.2 after
588 which the treatments were applied for four hours.
589
590 **Minimum Inhibitory Concentration (MIC).** MIC assays were performed in 96-well plates
591 in a total volume of 200 µl per well. Overnight PA14 cultures were diluted into MHB to an
592 OD_{600} of 0.002 and distributed into 96 well plates that contained increasing concentrations
593 of ciprofloxacin, nalidixic acid, carbenicillin, imipenem, trimethoprim, polymyxin B,
594 gentamicin, amikacin, tobramycin, streptomycin, and kanamycin, respectively. Plates
595 were subsequently incubated at 37 °C for 16 hours at 300 rpm. MIC assays were
596 performed in duplicates. The MIC is defined as the lowest antibiotic concentration that
597 inhibited growth.
598
599 **Time Killing Assays.** Overnight PA14 cultures were diluted ~25-fold into MHB by
600 normalizing cultures to an OD_{600} = 0.1 in a 6-well sterile cell culture plate. Sublethal
601 concentrations of AGXX720C® and antibiotics of interest were added individually and in
602 combination as indicated and plates incubated at 37°C for 3 hours at 150 rpm under
603 aerobic conditions. For thiourea, CCCP and BIP pretreatments, overnight PA14 was
604 grown in MOPSg to exponential phase. Thiourea, CCCP or BIP was then added 60
605 minutes prior to AGXX®/aminoglycoside treatments whenever indicated. At 1-hour
606 intervals, OD_{600} of cultures were recorded, sample volumes were normalized to the lowest
607 optical density measured, serially diluted in PBS (pH = 7.4) and plated on LB agar to
608 quantify colony forming units (CFU) after 16 hours incubation. Percent survival was
609 calculated as the ratio of surviving colonies from treated to untreated samples.
610
611 **Intracellular ROS level.** Intracellular ROS levels were quantified using the redox-
612 sensitive dye 2',7'-dichlorodihydrofluorescein diacetate (H_2DCFDA) (Thermofisher
613 Scientific). Exponentially growing PA14 cultures were left untreated or treated with 0.25
614 µg/ml Gm, 50 µg/ml AGXX720C® or a combination of both for 1 hour. Samples were
615 collected and normalized to an OD_{600}=1.0. Cells were washed twice, resuspended in
616 prewarmed PBS containing 10 µM H_2DCFDA, and incubated in the dark at 37 °C for 30
617 min before samples were washed twice again in PBS and DCF fluorescence measured

618 at excitation/emission wavelengths of 485/535 nm (Tecan 200 plate reader). To quench
619 cellular ROS, cells were pretreated with 50 mM thiourea prior to the stress treatments.
620
621 **Quantification of hydrogen peroxide level.** The monoborate fluorescent probe peroxy
622 orange 1 (PO1) was used to measure hydrogen peroxide level. Exponentially growing
623 PA14 cultures were treated with 10 µM PO1 prior to their exposure to 0.25 µg/ml Gm, 50
624 µg/ml AGXX720C®, or a combination of both for 1 hour. Cells were washed twice and
625 resuspended in prewarmed PBS. Samples were analyzed using the flow cytometer (BD
626 FACS Melody™) in the PE-CF594 channel. At least 10,000 events were recorded, and
627 figures generated using FCSalyzer (*77*).
628
629 **Quantification of Hydroxyl radical level.** The fluorescent probe hydroxyphenyl
630 fluorescein (HPF; Invitrogen) was used to determine the amount of cellular hydroxyl
631 radicals (•OH) produced (*33*). Exponentially growing PA14 cultures were either left
632 untreated or treated for 1 hour with 0.25 µg/ml Gm, 50 µg/ml AGXX720C®, or the
633 combination thereof. Samples were collected and normalized to an OD_{600nm} of 1.0 after
634 washing twice with PBS (pH 7.4). Cells were then stained with 10 µM HPF and incubated
635 in the dark for 30 minutes at 37 °C. Cells were washed twice and resuspended in
636 prewarmed PBS. Samples were analyzed using the flow cytometer (BD FACS Melody™)
637 in the FITC channel. At least 10,000 events were recorded, and figures generated using
638 FCSalyzer (*77*).
639
640 **Gene expression analyses by qRT-PCR.** Overnight PA14 cultures were diluted into
641 MOPSg media to an OD_{600}=0.1 and grown to mid-log phase (OD_{600nm}=0.3). Cultures were
642 left untreated or treated with 0.25 µg/ml Gm, 50 µg/ml AGXX720C®, or the combination
643 thereof for 60 minutes. Transcription was stopped by the addition of an equal volume of
644 ice-cold methanol. Total RNA was extracted from three biological replicates using a
645 commercially available RNA extraction kit (Macherey & Nagel). Remaining DNA was
646 removed using the TURBO DNA-free kit (Thermo Scientific). mRNA was reverse
647 transcribed into cDNA using the PrimeScript cDNA synthesis kit (Takara). The following
648 primer pairs were used for gene amplification:

649 *ibpA* - TTCCGTCATTCCGTAGG/ AGGTCTTCTTCCTGG ;
650 *sulA* - ACTGTTCCAGGAAGCGTTCT/ AGCGAAAGTTCGCTAAAGGC;
651 *rrsD* - TATCAGATGAGCCTAGGTCGGATTA/ TTTACAATCCGAAGACCTTCTTCAC.
652 qRT-PCRs were set up according to the manufacturer's instructions (Alkali Scientific).
653 Transcript levels of the indicated genes were normalized against transcript levels of the
654 16S rRNA-encoding *rrsD* gene and relative fold changes in gene expression were
655 calculated using the $2^{-\Delta\Delta CT}$ method(*78*).
656
657 **Aconitase Assay.** Exponentially growing PA14 were treated with sublethal
658 concentrations of AGXX720C® (100 μg/ml), Gm (0.6 μg/ml) or the combination thereof.
659 Aconitase activity was measured from cell lysates using the Aconitase Assay Kit (Abcam)
660 according to manufacturer's instructions. One unit of aconitase is defined as the amount
661 of enzyme that isomerizes 1 μmol of citrate to isocitrate per min at pH 7.4 and 25 °C.
662
663 **Outer membrane permeability assay.** The N-phenyl-1-naphthylamine (NPN) uptake
664 assay was used to detect outer membrane damage as described in (*79*). Exponential
665 phase PA14 were treated with 0.25 μg/ml Gm, 50 μg/ml AGXX720C®, a combination
666 thereof. Addition of 2 μg/ml polymyxin B was used as a positive control. Cells were
667 collected after 60 min of treatment, washed, and resuspended to an OD_{600}=0.5 in HEPES-
668 sodium buffer (pH 7.2). 10 μM NPN was added, and samples incubated in the dark for 15
669 min. NPN fluorescence was measured at excitation/emission wavelengths of 350/420 nm.
670 Increased NPN uptake (indicating outer membrane damage) was calculated using the
671 following equation (*80*):

672 $$NPN\ uptake = \frac{Sample_{+NPN} - Sample_{-NPN}}{Hepes\ Buffer_{+NPN} - Hepes\ Buffer_{-NPN}}$$

673
674 **Inner membrane disruption assay.** Inner membrane integrity was determined by the
675 cellular uptake of propidium iodide following antimicrobial treatments. Exponentially
676 growing PA14 cells were either left untreated or treated with 0.25 μg/ml Gm, 50 μg/ml
677 AGXX720C®, or a combination thereof. Cells were harvested after 1 hour, washed twice,
678 and resuspended in PBS (pH 7.4) at an OD_{600}=0.5. Propidium iodide (Thermo Fisher

679 Scientific) was added to a final concentration of 500 nM and samples incubated in the
680 dark for 30 min. Fluorescence intensities were measured at excitation/emission
681 wavelengths of 535/617 nm. Samples treated with polymyxin B at a sublethal
682 concentration (2 μg/ml) were included as a positive control.
683
684 **LIVE/DEAD staining.** Exponentially growing PA14 cells were either left untreated or
685 treated with 0.25 µg/ml Gm, 50 µg/ml AGXX720C®, or a combination thereof. Cells were
686 harvested after 1 hour, washed twice, and resuspended in PBS (pH 7.4) at an OD_{600}=0.2.
687 Samples were stained with SYTO9 (6µM) and PI (30 µM) and incubated in the dark for
688 15 min at room temperature**.** Cells were then transferred onto a glass slide and covered
689 with 1% agarose prior to visualization using a Leica SP8 confocal system equipped with
690 a DMi8 CS inverted microscope. Samples treated with polymyxin B at a sublethal
691 concentration (2 μg/ml) were included as a positive control.
692
693 **Texas Red-Gentamicin Uptake Assay**. Texas Red-succinimidyl ester (Invitrogen) was
694 dissolved to a final concentration of 20 mg/ml in high quality anhydrous N,N-
695 dimethylformamide at 4 °C (*81*). Gm was dissolved in 100 mM K_2CO_3 (pH 8.5) to a final
696 concentration of 10 mg/ml at 4 °C. 20 µl Texas Red was slowly added dropwise to 700 ul
697 Gm to allow for the conjugation reaction to obtain the Texas-Red labeled gentamicin (TR-
698 Gm) (*81*). The TR-Gm conjugate was diluted in water and stored at -20 °C protected from
699 light. Exponentially growing PA14 cells were first treated with 1 µg/ml TR-Gm followed by
700 exposure to either 50 µg/ml AGXX720C® or 2 µg/ml polymyxin B (positive control). After
701 1 hour incubation in the dark at 37 °C, cells were collected and analyzed in the flow
702 cytometer (BD FACS Melody™) using the PE-Cy5 channel. At least 10,000 events were
703 recorded, and figures generated using FCSalyzer (*77*).
704
705 **Statistical analyses:** All statistical analyses were performed in GraphPad prism version
706 8.0.
707

ACKNOWLEDGEMENTS

This work was supported by the NIAID grant R15AI164585 and the Illinois State University Pre-Tenure Faculty Initiative Grant (to J.-U. D.). G.Y.D. was supported by Weigel and Mockford-Thompson by the Phi-Sigma Biological Sciences Honors Society, and the SIGMA Xi and BIRDFeeder grants. G.M.A. and C.D.O. were supported by the Illinois State University Undergraduate Research Support Program. Dr. Uwe Landau and his team from Largentec GmbH are acknowledged for scientific discussion and providing the AGXX® formulations. We further thank the ISU Confocal Microscopy Facility which was funded by NSF grant DBI-1828136, for their support. We also thank Sadia Sultana for critically proof-reading the manuscript and providing invaluable feedback. Figure 9 was generated with Adobe Illustrator.

FIGURE LEGENDS

FIG 1 AGXX394® is more efficient in killing *P. aeruginosa* than silverdene and silver nitrate. Overnight PA14 cultures were diluted ~25-fold into MOPSg media (OD_{600} = 0.1) and treated for three hours with 25 µg/ml $AgNO_3$ (black square), silverdene (grey square), and AGXX394® (red square), respectively. Colony survival was evaluated every hour by serially diluting samples and plating them onto LB agar. Percent survival was calculated relative to the untreated control (*n=4, ± S.D).*

FIG 2 AGXX® exponentially increases the activity of aminoglycosides against *P. aeruginosa*. In our time killing assay, overnight PA14 cultures were diluted ~25-fold (OD600 = 0.1) into MHB and exposed to 75 µg/ml AGXX720C® (black bars), a sublethal concentration of the indicated antibiotic (grey bar), or the combined treatment of both (red bars) for 3 hours. Samples were taking every 60 min, serial diluted, plated on LB agar, and incubated for 20 hours for CFU counts. Percent survival was calculated relative to the untreated control for: (A) 35 ng/ml ciprofloxacin and 100 ng/ml nalidixic acid, respectively; (B) 78 µg/ml carbenicillin and 0.156 µg/ml imipenem, respectively; (C) 125 µg/ml trimethoprim; (D) 1.5 µg/ml polymyxin B; and (E) 0.4 µg/ml gentamicin, 2.0 µg/ml amikacin, 1.0 µg/ml tobramycin, and 3 µg/ml streptomycin, respectively. All experiments

739 were performed in at least three biological replicates and error bars represent mean (±
740 SD. * $p < 0.05$, ** $p < 0.01$, *** $p < 0.001$; student's t test, calculated relative to cultures
741 treated with antibiotics alone).
742
743 **FIG 3 AGXX® increases the sensitivity of *P. aeruginosa* strain PA14 to kanamycin.**
744 Overnight PA14 cultures were diluted ~25-fold into Mueller-Hinton media (OD_{600}=0.1) and
745 either left untreated or exposed to 75 µg/ml AGXX720C®, 50 µg/ml kanamycin, or the
746 combination thereof for 3 hours. Samples were taken every 60 minutes, serial diluted and
747 plated on LB agar for CFU counts, (*n=4, ± S.D)*.
748
749 **FIG 4 The combination of sublethal concentrations of AGXX® and gentamicin**
750 **increases ROS levels and causes DNA damage and protein aggregation.** Mid-log
751 PA14 cells were treated with sublethal concentrations of Gm (0.25 µg/ml), AGXX720C®
752 (50 µg/ml), the combination thereof, or left untreated. **(A)** Intracellular ROS levels were
753 quantified by H_2DCFDA fluorescence. 50mM thiourea was used as a ROS quencher (*n=3,*
754 *± S.D.)*. **(B)** Samples were serially diluted in PBS after 60 min of incubation, spot-titered
755 onto LB agar and incubated for 20 hours. One representative of three independent
756 experiments with similar outcomes. **(C, D)** Cells were strained with **(C)** 10 µM peroxy-
757 orange 1 (PO1) and **(D)** 10µM hydroxyphenyl fluorescein (HPF) for 60 min and
758 fluorescence was measured via flow cytometry (*n=3, ± S.D.)*. **(E)** The induction of *sulA*
759 (white bar) and *ibpA* (black bar) transcript levels was determined by qRT-PCR. Gene
760 expression was normalized to the housekeeping gene *rrsD* and calculated as fold
761 changes based on expression levels in the untreated control (*n=3, ± S.D.*; One-way
762 ANOVA, Dunnett's posttest; *ns=p>0.05,* * $p < 0.05$, ** $p < 0.01$, *** $p < 0.001$, **** $p <$
763 0.0001).
764
765 **FIG 5 Anaerobic growth and antioxidant systems provide protection against ROS-**
766 **mediated damage caused by a combinational treatment of AGXX® and**
767 **aminoglycosides. (A)** PA14 were diluted approximately 1000-fold (OD_{600}=0.002) in MHB
768 supplemented with 1% KNO_3 and grown under aerobic (black bars) and anaerobic (grey
769 bars) conditions, respectively. At OD_{600} ~0.2, cultures were treated with either 0.5 µg/ml

770 or 1.0 µg/ml Gm alone or in combination with 75 µg/ml AGXX® for four hours. Cells were
771 subsequently plated onto LB agar for 20 hours at 37°C to enumerate surviving colonies
772 (*n=3,* ± *S.D.*). **(B)** Overnight cultures of PA14 wildtype and mutant strains with MrT7
773 transposon insertions in *oxyR, katA, katB* and *dps* were diluted into MOPSg to an
774 OD_{600}=0.01 and grown under aerobic conditions until OD_{600}=0.1. Cultures were either left
775 untreated (grey bars) or treated with a combination of 0.25 µg/ml tobramycin and 25 µg/ml
776 AGXX720C® (white bars). Bacterial survival was quantified after two hours by serially
777 diluting cells in PBS and plating on LB agar for 20 hours at 37°C (*n=3,* ± *S.D*; Student t-
778 test, * $p < 0.05$).
779
780 **FIG 6 The synergy between AGXX® and aminoglycosides on PA14 killing is in parts**
781 **mediated by a disruption in iron homeostasis.** Overnight PA14 cultures were diluted
782 into MOPSg and incubated under aerobic conditions until exponential phase was
783 reached. **(A)** Cells were left untreated or treated with 100 µg/ml AGXX720C®, 0.6 µg/ml
784 Gm, or the combination thereof for 1 hour. Aconitase activities were determined in crude
785 extracts (*n=4,* ± *S.D*). One-way ANOVA, Dunnett's posttest; *ns* $p>0.05$, ** $p < 0.01$. **(B)**
786 Cultures were either left untreated (white square) or treated with 0.25 µg/ml Gm (white
787 diamond), 50µg/ml AGXX720C® (white circle), or the combination thereof (white triangle)
788 for three hours. Survival was determined each hour by serially diluting samples in PBS
789 and plating onto LB agar for overnight growth. The impact of free iron on the increased
790 killing by AGXX®/Gm cotreatments was tested by the absence (white triangle) and
791 presence (black diamonds) of 125 µM 2',2' bipyridyl (*n=3,* ± *S.D.*). Student's t test, *
792 $p<0.05$).
793
794 **FIG 7 Combined AGXX® and aminoglycoside treatment induces significant**
795 **membrane damage.** PA14 cells grown to mid-log phase in MOPSg media were left
796 untreated or treated with sublethal concentrations of Gm (0.25 µg/ml), AGXX720C® (50
797 µg/ml), and the combination thereof. Cells were harvested after 1 hour of treatment,
798 washed in PBS, and stained with **(A)** 10 µM N-phenyl-1-naphthylamine (NPN) dye, and
799 **(B)** 0.5 µM propidium iodide (PI). Fluorescence intensities were determined at
800 excitation/emission wavelengths of **(A)** 350/420 nm and **(B)** 535/617 nm, respectively,

801 (*n=4, ± S.D.*). One-way ANOVA, Dunnett's posttest; *ns p>0.05, * p* < 0.05, **** *p* < 0.0001.
802 **(C)** Samples were washed in PBS, stained with PI/Syto9, incubated in the dark for 15
803 minutes at room temperature, mounted onto a glass slide with 1% agarose, and imaged
804 at 63x magnification via inverted confocal microscopy. One representative of three
805 independent experiments with similar outcomes.
806
807 **FIG 8 AGXX® increases aminoglycoside uptake and lethality through increased**
808 **activity of the proton motive force (PMF). (A)** Mid-log PA14 cells were treated with 1.0
809 µg/ml TR-Gm, 1.0 µg/ml TR-Gm + 50 µg/ml AGXX720C®, and 1.0 µg/ml TR-Gm + 2.0
810 µg/ml polymyxin B (PMB) for 1 hour, respectively. TR-Gm uptake was measured via flow
811 cytometry. **(B)** Mid-log phase PA14 were left untreated (control) or exposed to 0.25 µg/ml
812 Gm, 50 µg/ml AGXX720C® or 0.25 µg/ml Gm + 50 µg/ml AGXX720C® for 3 hours.
813 Samples were serial diluted, plated on LB agar, and incubated for 20 hours for CFU
814 counts. To test the impact of the PMF on the killing of a combination of AGXX® and
815 aminoglycosides, PA14 were pretreated with or without 50 µM carbonyl cyanide *m*-
816 chlorophenyl hydrazone (CCCP) prior to AGXX®/Gm exposure *(n=3, ± S.D.)*. Student's t
817 test, ** *p*<0.01.
818
819 **FIG 9 Proposed model for the synergy between AGXX® and aminoglycoside**
820 **antibiotics.** The antimicrobial action of AGXX® is mediated by superoxide (O_2^-) and
821 hydrogen peroxide (H_2O_2), which are generated in a redox cycle between silver (Ag) and
822 ruthenium (Ru^{x+1}). The combination of AGXX® and aminoglycosides concertedly
823 increases endogenous ROS levels. As such anaerobic growth suppressed the synergistic
824 interaction between the two antimicrobials at lower Gm concentrations. Potentially
825 facilitated by a release of silver ions, the increased ROS level may disrupt iron-sulfur
826 clusters in metabolic enzymes such as aconitase, resulting in the release of free iron,
827 which ultimately triggers hydroxyl radical (•OH) formation in a Fenton reaction. Increasing
828 ROS levels can inflict macromolecule damage such as DNA damage and protein
829 aggregation, contributing to increased killing as observed for *P. aeruginosa* that were
830 treated with a combination of AGXX® and aminoglycosides. The synergistic effect
831 between AGXX® and aminoglycosides is also mediated by an increased uptake and the

832 cellular accumulation of aminoglycosides, which can be attenuated by disrupting the
833 bacterial membrane potential with ionophores such as CCCP.
834

References

1. C. Llor, L. Bjerrum, Antimicrobial resistance: risk associated with antibiotic overuse and initiatives to reduce the problem. *Ther. Adv. Drug Saf.* **5**, 229–41 (2014).

2. B. Spellberg, The future of antibiotics. *Crit. Care*. **18**, 228 (2014).

3. K. H. Turner, J. Everett, U. Trivedi, K. P. Rumbaugh, M. Whiteley, Requirements for Pseudomonas aeruginosa Acute Burn and Chronic Surgical Wound Infection. *PLOS Genet.* **10**, e1004518 (2014).

4. Z. Pang, R. Raudonis, B. R. Glick, T. J. Lin, Z. Cheng, Antibiotic resistance in Pseudomonas aeruginosa: mechanisms and alternative therapeutic strategies. *Biotechnol. Adv.* **37**, 177–192 (2019).

5. I. Chopra, L. Hesse, A. J. O'Neill, Exploiting current understanding of antibiotic action for discovery of new drugs. *Symp. Ser. Soc. Appl. Microbiol.* **31**, 4S-15S (2002).

6. D. Shang, Y. Liu, F. Jiang, F. Ji, H. Wang, X. Han, Synergistic Antibacterial Activity of Designed Trp-Containing Antibacterial Peptides in Combination With Antibiotics Against Multidrug-Resistant Staphylococcus epidermidis. *Front. Microbiol.* **0**, 2719 (2019).

7. F. Barras, L. Aussel, B. Ezraty, Silver and antibiotic, new facts to an old story. *Antibiotics*. **7**, 1–10 (2018).

8. S. Georgios A, P. Sotiris E, Antibacterial activity of nanosilver ions and particles. *Environ. Sci. Technol.* **44**, 5649–5654 (2010).

9. S. Y. Liau, D. C. Read, W. J. Pugh, J. R. Furr, A. D. Russell, Interaction of silver nitrate with readily identifiable groups: Relationship to the antibacterial action of silver ions. *Lett. Appl. Microbiol.* **25**, 279–283 (1997).

10. F. F. Xu, J. A. Imlay, Silver(I), Mercury(II), Cadmium(II), and Zinc(II) Target Exposed Enzymic Iron-Sulfur Clusters when They Toxify Escherichia coli. *Appl. Environ. Microbiol.* **78**, 3614 (2012).

11. D. Church, S. Elsayed, O. Reid, B. Winston, R. Lindsay, Burn wound infections. *Clin. Microbiol. Rev.* **19**, 403–434 (2006).

12. E. Clauss-Lendzian, A. Vaishampayan, A. de Jong, U. Landau, C. Meyer, J. Kok, E. Grohmann, Stress response of a clinical Enterococcus faecalis isolate subjected to a novel antimicrobial surface coating. *Microbiol. Res.* **207**, 53–64 (2018).

13. V. V. Loi, T. Busche, T. Preuß, J. Kalinowski, J. Bernhardt, H. Antelmann, The AGXX® Antimicrobial Coating Causes a Thiol-Specific Oxidative Stress Response

and Protein S-bacillithiolation in Staphylococcus aureus. *Front. Microbiol.* **9**, 3037 (2018).

14. L.-Y. Sobisch, K. M. Rogowski, J. Fuchs, W. Schmieder, A. Vaishampayan, P. Oles, N. Novikova, E. Grohmann, Biofilm Forming Antibiotic Resistant Gram-Positive Pathogens Isolated From Surfaces on the International Space Station. *Front. Microbiol.* **10**, 543 (2019).

15. N. Linzner, H. Antelmann, The Antimicrobial Activity of the AGXX® Surface Coating Requires a Small Particle Size to Efficiently Kill Staphylococcus aureus. *Front. Microbiol.* **12** (2021), doi:10.3389/FMICB.2021.731564/FULL.

16. A. Guridi, A. K. Diederich, S. Aguila-Arcos, M. Garcia-Moreno, R. Blasi, M. Broszat, W. Schmieder, E. Clauss-Lendzian, T. Sakinc-Gueler, R. Andrade, I. Alkorta, C. Meyer, U. Landau, E. Grohmann, New antimicrobial contact catalyst killing antibiotic resistant clinical and waterborne pathogens. *Mater. Sci. Eng. C*. **50**, 1–11 (2015).

17. J. Ruben Morones-Ramirez, J. A. Winkler, C. S. Spina, J. J. Collins, Silver enhances antibiotic activity against gram-negative bacteria. *Sci. Transl. Med.* **5** (2013), doi:10.1126/scitranslmed.3006276.

18. L. Kalan, G. D. Wright, Antibiotic adjuvants: multicomponent anti-infective strategies. *Expert Rev. Mol. Med.* **13** (2011), doi:10.1017/S1462399410001766.

19. A. Huttner, J. Bielicki, M. N. Clements, N. Frimodt-Møller, A. E. Muller, J.-P. Paccaud, J. W. Mouton, Oral amoxicillin and amoxicillin–clavulanic acid: properties, indications and usage. *Clin. Microbiol. Infect.* **26**, 871–879 (2020).

20. M. P. Brynildsen, J. A. Winkler, C. S. Spina, I. C. MacDonald, J. J. Collins, Potentiating antibacterial activity by predictably enhancing endogenous microbial ROS production. *Nat. Biotechnol.* **31**, 160 (2013).

21. J. J. Foti, B. Devadoss, J. A. Winkler, J. J. Collins, G. C. Walker, Oxidation of the guanine nucleotide pool underlies cell death by bactericidal antibiotics. *Science*. **336**, 315–319 (2012).

22. G. Soothill, Y. Hu, A. Coates, Can We Prevent Antimicrobial Resistance by Using Antimicrobials Better? *Pathog. 2013 Vol 2 Pages 422-435*. **2**, 422–435 (2013).

23. Q. L. Feng, J. Wu, G. Q. Chen, F. Z. Cui, T. N. Kim, J. O. Kim, A mechanistic study of the antibacterial effect of silver ions on Escherichia coli and Staphylococcus aureus. *J. Biomed. Mater. Res.* **52**, 662–668 (2000).

24. S. Silver, L. T. Phung, G. Silver, Silver as biocides in burn and wound dressings and bacterial resistance to silver compounds. *J. Ind. Microbiol. Biotechnol.* **33**, 627–634 (2006).

25. S. Egger, R. P. Lehmann, M. J. Height, M. J. Loessner, M. Schuppler, Antimicrobial Properties of a Novel Silver-Silica Nanocomposite Material. *Appl. Environ. Microbiol.* **75**, 2973–2976 (2009).

26. F. W. Fuller, The side effects of silver sulfadiazine. *J. Burn Care Res. Off. Publ. Am. Burn Assoc.* **30**, 464–470 (2009).

27. H. Kim, X. Xue, Detection of Total Reactive Oxygen Species in Adherent Cells by 2',7'-Dichlorodihydrofluorescein Diacetate Staining. *J. Vis. Exp. JoVE*. **2020**, 1–5 (2020).

28. M. Herisse, Y. Duverger, I. Martin-Verstraete, F. Barras, B. Ezraty, Silver potentiates aminoglycoside toxicity by enhancing their uptake. *Mol. Microbiol.* **105**, 115–126 (2017).

29. M. A. Kohanski, A. Tharakan, A. P. Lane, M. Ramanathan, Bactericidal Antibiotics Promote Reactive Oxygen Species Formation and Inflammation in Human Sinonasal Epithelial Cells. *Int. Forum Allergy Rhinol.* **6**, 191 (2016).

30. M. A. Kohanski, D. J. Dwyer, B. Hayete, C. A. Lawrence, J. J. Collins, A Common Mechanism of Cellular Death Induced by Bactericidal Antibiotics. *Cell*. **130**, 797–810 (2007).

31. M. J. Kelner, R. Bagnell, K. J. Welch, Thioureas react with superoxide radicals to yield a sulfhydryl compound. Explanation for protective effect against paraquat. *J. Biol. Chem.* **265**, 1306–1311 (1990).

32. B. C. Dickinson, C. Huynh, C. J. Chang, A Palette of Fluorescent Probes with Varying Emission Colors for Imaging Hydrogen Peroxide Signaling in Living Cells. *J. Am. Chem. Soc.* **132**, 5906 (2010).

33. M. Price, J. J. Reiners, A. M. Santiago, D. Kessel, Monitoring Singlet Oxygen and Hydroxyl Radical Formation with Fluorescent Probes During Photodynamic Therapy. *Photochem. Photobiol.* **85**, 1177–1181 (2009).

34. S. Sultana, J.-U. Dahl, A Year at the Forefront of Bacterial Defense Systems Against Neutrophilic Oxidants. *Biol. Open*. **12**, bio059809 (2023).

35. S. Sultana, A. Foti, J.-U. Dahl, Bacterial Defense Systems against the Neutrophilic Oxidant Hypochlorous Acid. *Infect. Immun.* **88** (2020), doi:10.1128/IAI.00964-19.

36. M. Varatnitskaya, A. Degrossoli, L. I. Leichert, Redox regulation in host-pathogen interactions: thiol switches and beyond. *Biol. Chem.* **402**, 299–316 (2021).

37. A. Sen, J. A. Imlay, How Microbes Defend Themselves From Incoming Hydrogen Peroxide. *Front. Immunol.* **12**, 667343 (2021).

38. M. J. Gray, W.-Y. Wholey, U. Jakob, Bacterial Responses to Reactive Chlorine Species. *Annu. Rev. Microbiol.* **67**, 141–160 (2013).

39. J.-U. Dahl, M. J. Gray, U. Jakob, Protein Quality Control under Oxidative Stress Conditions. *J. Mol. Biol.* **427**, 1549–1563 (2015).

40. B. Ezraty, A. Gennaris, F. Barras, J. F. Collet, Oxidative stress, protein damage and repair in bacteria. *Nat. Rev. Microbiol. 2017 157*. **15**, 385–396 (2017).

41. M. S. Cooke, M. D. Evans, M. Dizdaroglu, J. Lunec, Oxidative DNA damage: mechanisms, mutation, and disease. *FASEB J.* **17**, 1195–1214 (2003).

42. B. Groitl, J.-U. Dahl, J. W. Schroeder, U. Jakob, Pseudomonas aeruginosa defense systems against microbicidal oxidants. *Mol. Microbiol.* **106**, 335–350 (2017).

43. S. Sultana, M. E. Crompton, K. Meurer, O. Jankiewicz, G. H. Morales, C. Johnson, E. Horbach, K. P. Hoffmann, P. Kr, R. Shah, G. M. Anderson, N. T. Mortimer, J. E. Schmitz, M. Hadjifrangiskou, A. Foti, J.-U. Dahl, Redox-Mediated Inactivation of the Transcriptional Repressor RcrR is Responsible for Uropathogenic Escherichia coli's Increased Resistance to Reactive Chlorine Species. *mBio*. **13**, e01926-22 (2022).

44. M. Kitagawa, Y. Matsumura, T. Tsuchido, Small heat shock proteins, IbpA and IbpB, are involved in resistances to heat and superoxide stresses in Escherichia coli. *FEMS Microbiol. Lett.* **184**, 165–171 (2000).

45. K. Lewis, Programmed Death in Bacteria. *Microbiol. Mol. Biol. Rev.* **64**, 503–514 (2000).

46. N. T. Liberati, J. M. Urbach, S. Miyata, D. G. Lee, E. Drenkard, G. Wu, J. Villanueva, T. Wei, F. M. Ausubel, An ordered, nonredundant library of Pseudomonas aeruginosa strain PA14 transposon insertion mutants. *Proc. Natl. Acad. Sci.* **103**, 2833–2838 (2006).

47. K. Keyer, J. A. Imlay, Superoxide accelerates DNA damage by elevating free-iron levels. *Proc. Natl. Acad. Sci. U. S. A.* **93**, 13635–13640 (1996).

48. S. I. Liochev, I. Fridovich, The role of O2.- in the production of HO.: in vitro and in vivo. *Free Radic. Biol. Med.* **16**, 29–33 (1994).

49. H. W. Taber, J. P. Mueller, P. F. Miller, A. S. Arrow, Bacterial uptake of aminoglycoside antibiotics. *Microbiol. Rev.* **51**, 439–457 (1987).

50. W. Kim, W. Zhu, G. L. Hendricks, D. Van Tyne, A. D. Steele, C. E. Keohane, N. Fricke, A. L. Conery, S. Shen, W. Pan, K. Lee, R. Rajamuthiah, B. B. Fuchs, P. M. Vlahovska, W. M. Wuest, M. S. Gilmore, H. Gao, F. M. Ausubel, E. Mylonakis, A new class of synthetic retinoid antibiotics effective against bacterial persisters. *Nat. 2018 5567699*. **556**, 103–107 (2018).

51. D. Pletzer, S. C. Mansour, R. E. W. Hancock, Synergy between conventional antibiotics and anti-biofilm peptides in a murine, sub-cutaneous abscess model caused by recalcitrant ESKAPE pathogens. *PLOS Pathog.* **14**, e1007084 (2018).

52. C. R. MacNair, J. M. Stokes, L. A. Carfrae, A. A. Fiebig-Comyn, B. K. Coombes, M. R. Mulvey, E. D. Brown, Overcoming mcr-1 mediated colistin resistance with colistin in combination with other antibiotics. *Nat. Commun. 2018 91*. **9**, 1–8 (2018).

53. D. J. Arndt-Jovin, T. M. Jovin, Chapter 16 Fluorescence Labeling and Microscopy of DNA. *Methods Cell Biol.* **30**, 417–448 (1989).

54. L. E. Bryan, H. M. Van Den Elzen, Streptomycin accumulation in susceptible and resistant strains of Escherichia coli and Pseudomonas aeruginosa. *Antimicrob. Agents Chemother.* **9**, 928–938 (1976).

55. S. Meylan, C. B. M. Porter, J. H. Yang, P. Belenky, A. Gutierrez, M. A. Lobritz, J. Park, S. H. Kim, S. M. Moskowitz, J. J. Collins, S. M. Conceptualization, J. J. C. ; Methodology, J. J. C. Investigation, F. Acquisition, J. J. C. ; Resources, S. M. M. ; Supervision, Carbon Sources Tune Antibiotic Susceptibility in Pseudomonas aeruginosa via Tricarboxylic Acid Cycle Control HHS Public Access. *Cell Chem Biol*. **24**, 195–206 (2017).

56. S. I. Liochev, The mechanism of “Fenton-like” reactions and their importance for biological systems. A biologist’s view. *undefined*. **36**, 1–39 (1999).

57. B. Nowack, H. F. Krug, M. Height, 120 years of nanosilver history: implications for policy makers. *Environ. Sci. Technol.* **45**, 1177–1183 (2011).

58. W. K. Jung, H. C. Koo, K. W. Kim, S. Shin, S. H. Kim, Y. H. Park, Antibacterial Activity and Mechanism of Action of the Silver Ion in Staphylococcus aureus and Escherichia coli. *Appl. Environ. Microbiol.* **74**, 2171–2178 (2008).

59. R. B.-K. Wakshlak, R. Pedahzur, D. Avnir, Antibacterial activity of silver-killed bacteria: the “zombies” effect. *Sci. Rep.* **5**, 9555 (2015).

60. A. Panáček, L. Kvítek, M. Smékalová, R. Večeřová, M. Kolář, M. Röderová, F. Dyčka, M. Šebela, R. Prucek, O. Tomanec, R. Zbořil, Bacterial resistance to silver nanoparticles and how to overcome it. *Nat. Nanotechnol. 2017 131*. **13**, 65–71 (2017).

61. H. Wang, M. Wang, X. Xu, P. Gao, Z. Xu, Q. Zhang, H. Li, A. Yan, R. Y. T. Kao, H. Sun, Multi-target mode of action of silver against Staphylococcus aureus endows it with capability to combat antibiotic resistance. *Nat. Commun. 2021 121*. **12**, 1–16 (2021).

62. R. Tambosi, S. Liotenberg, M.-L. Bourbon, A.-S. Steunou, M. Babot, A. Durand, N. Kebaili, S. Ouchane, Silver and Copper Acute Effects on Membrane Proteins and

Impact on Photosynthetic and Respiratory Complexes in Bacteria. *mBio*. **9**, e01535-18 (2018).

63. A. Vaishampayan, A. de Jong, D. J. Wight, J. Kok, E. Grohmann, A novel antimicrobial coating represses biofilm and virulence-related genes in methicillin-resistant Staphylococcus aureus. *Front. Microbiol.* **9**, 1–14 (2018).

64. D. J. Dwyer, P. A. Belenky, J. H. Yang, I. Cody MacDonald, J. D. Martell, N. Takahashi, C. T. Y. Chan, M. A. Lobritz, D. Braff, E. G. Schwarz, J. D. Ye, M. Pati, M. Vercruysse, P. S. Ralifo, K. R. Allison, A. S. Khalil, A. Y. Ting, G. C. Walker, J. J. Collins, Antibiotics induce redox-related physi. *Proc. Natl. Acad. Sci. U. S. A.* **111**, E2100–E2109 (2014).

65. J. Ling, C. Cho, L.-T. Guo, H. Aerni, J. Rinehart, D. Söll, Protein aggregation caused by aminoglycoside action is prevented by a hydrogen peroxide scavenger. *Mol. Cell*. **48**, 713–722 (2012).

66. J. Ye, Y. Su, X. Lin, S. Lai, W. Li, F. Ali, J. Zheng, B. Peng, Alanine Enhances Aminoglycosides-Induced ROS Production as Revealed by Proteomic Analysis. *Front. Microbiol.* **9** (2018) (available at https://www.frontiersin.org/articles/10.3389/fmicb.2018.00029).

67. X. Ji, J. Zou, H. Peng, A.-S. Stolle, R. Xie, H. Zhang, B. Peng, J. J. Mekalanos, J. Zheng, Alarmone Ap4A is elevated by aminoglycoside antibiotics and enhances their bactericidal activity. *Proc. Natl. Acad. Sci.* **116**, 9578–9585 (2019).

68. S. Sultana, G. M. Anderson, K. P. Hoffmann, J.-U. Dahl, Extraction and Visualization of Protein Aggregates after Treatment of Escherichia coli with a Proteotoxic Stressor. *JoVE J. Vis. Exp.*, e62628 (2021).

69. B. Lv, X. Huang, C. Lijia, Y. Ma, M. Bian, Z. Li, J. Duan, F. Zhou, B. Yang, X. Qie, Y. Song, T. K. Wood, X. Fu, Heat shock potentiates aminoglycosides against gram-negative bacteria by enhancing antibiotic uptake, protein aggregation, and ROS. *Proc. Natl. Acad. Sci.* **120**, e2217254120 (2023).

70. J. A. Imlay, *How oxygen damages microbes: Oxygen tolerance and obligate anaerobiosis* (2002), vol. 46.

71. S. Park, X. You, J. A. Imlay, Substantial DNA damage from submicromolar intracellular hydrogen peroxide detected in Hpx- mutants of Escherichia coli. *Proc. Natl. Acad. Sci.* **102**, 9317–9322 (2005).

72. K. Poole, Pseudomonas aeruginosa: Resistance to the max. *Front. Microbiol.* **2**, 65 (2011).

73. R. E. W. Hancock, S. W. Farmer, Z. Li, K. Poole, Interaction of aminoglycosides with the outer membranes and purified lipopolysaccharide and OmpF porin of Escherichia coli. *Antimicrob. Agents Chemother.* **35**, 1309–1314 (1991).

74. R. E. Hancock, V. J. Raffle, T. I. Nicas, Involvement of the outer membrane in gentamicin and streptomycin uptake and killing in Pseudomonas aeruginosa. *Antimicrob. Agents Chemother.* **19**, 777–785 (1981).

75. G. D. Wright, Antibiotic Adjuvants: Rescuing Antibiotics from Resistance. *Trends Microbiol.* **24**, 862–871 (2016).

76. M. Wu, T. Guina, M. Brittnacher, H. Nguyen, J. Eng, S. I. Miller, The Pseudomonas aeruginosa Proteome during Anaerobic Growth. *J. Bacteriol.* **187**, 8185–8190 (2005).

77. Mostböck, Sven, FCSalyzer. *SourceForge* (2021), (available at https://sourceforge.net/projects/fcsalyzer/).

78. M. W. Pfaffl, A new mathematical model for relative quantification in real-time RT–PCR. *Nucleic Acids Res.* **29**, e45 (2001).

79. I. M. Helander, T. Mattila-Sandholm, Fluorometric assessment of Gram-negative bacterial permeabilization. *J. Appl. Microbiol.* **88**, 213–219 (2000).

80. A. Sabnis, K. L. H. Hagart, A. Klöckner, M. Becce, L. E. Evans, R. C. D. Furniss, D. A. I. Mavridou, R. Murphy, M. M. Stevens, J. C. Davies, G. J. Larrouy-Maumus, T. B. Clarke, A. M. Edwards, Colistin kills bacteria by targeting lipopolysaccharide in the cytoplasmic membrane. *eLife*. **10** (2021), doi:10.7554/ELIFE.65836.

81. H. Saito, K. Inui, R. Hori, Mechanisms of gentamicin transport in kidney epithelial cell line (LLC-PK1). *J. Pharmacol. Exp. Ther.* **238** (1986).

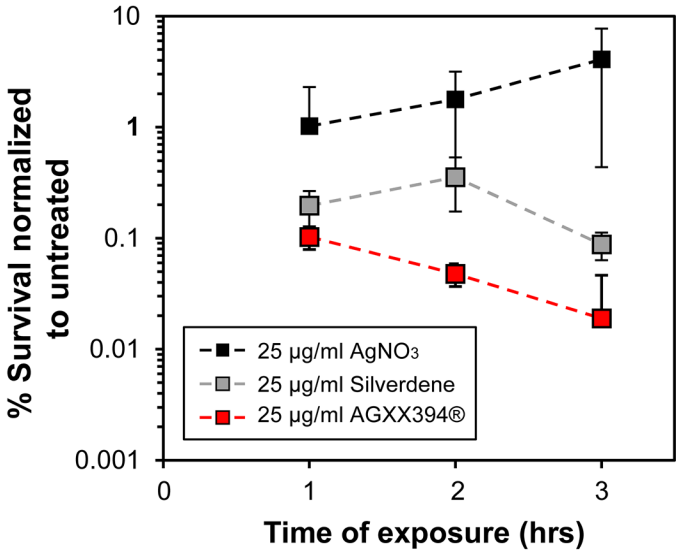

FIG 1 AGXX394® is more efficient in killing *P. aeruginosa* than silverdene and silver nitrate. Overnight PA14 cultures were diluted ~25-fold into MOPSg media (OD_{600} = 0.1) and treated for three hours with 25 µg/ml $AgNO_3$ (black square), silverdene (grey square), and AGXX394® (red square), respectively. Colony survival was evaluated every hour by serially diluting samples and plating them onto LB agar. Percent survival was calculated relative to the untreated control (*n=4, ± S.D).*

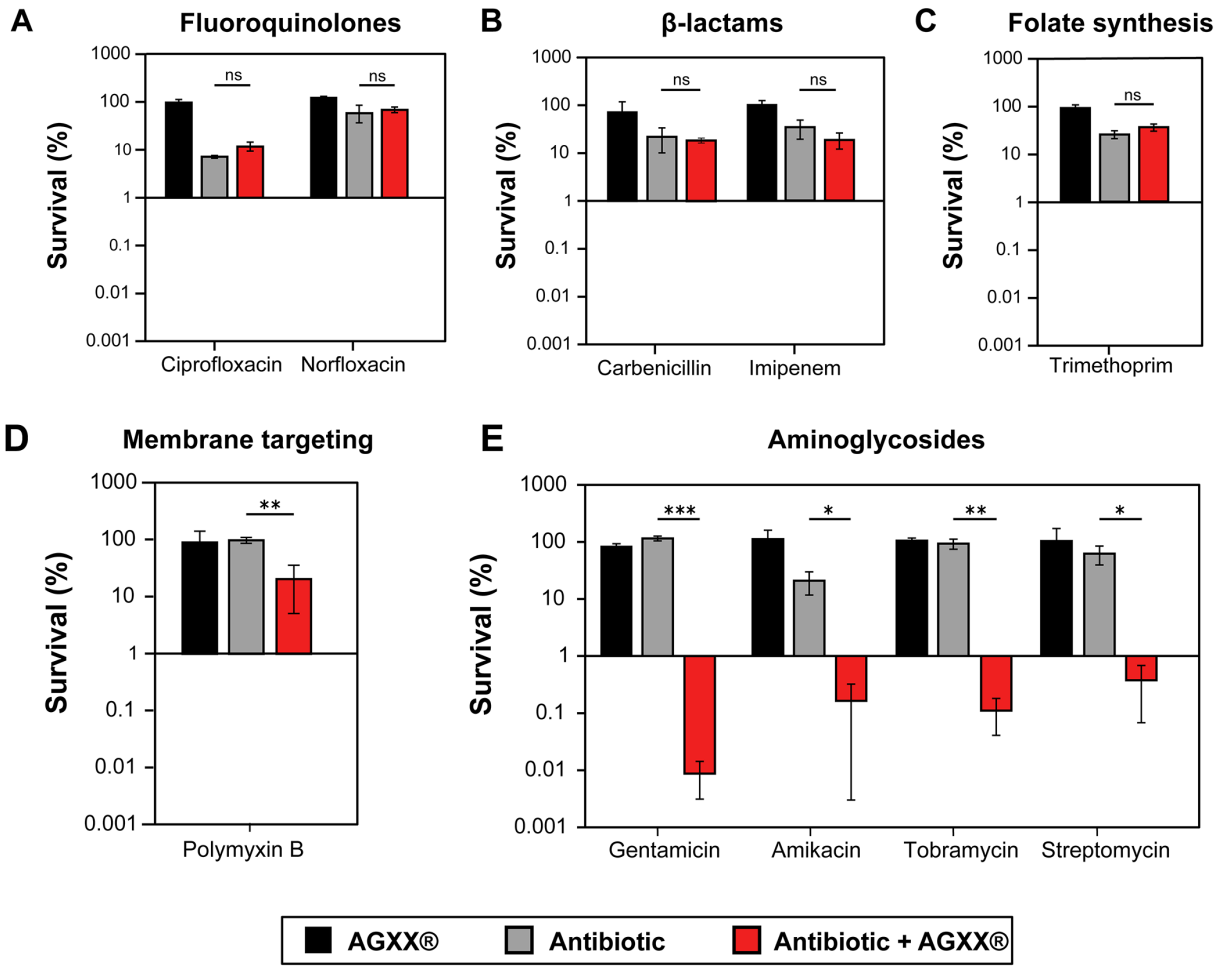

FIG 2 AGXX® exponentially increases the activity of aminoglycosides against *P. aeruginosa*. In our time killing assay, overnight PA14 cultures were diluted ~25-fold (OD600 = 0.1) into MHB and exposed to 75 µg/ml AGXX720C® (black bars), a sublethal concentration of the indicated antibiotic (grey bar), or the combined treatment of both (red bars) for 3 hours. Samples were taking every 60 min, serial diluted, plated on LB agar, and incubated for 20 hours for CFU counts. Percent survival was calculated relative to the untreated control for: (A) 35 ng/ml ciprofloxacin and 100 ng/ml nalidixic acid, respectively; (B) 78 µg/ml carbenicillin and 0.156 µg/ml imipenem, respectively; (C) 125 µg/ml trimethoprim; (D) 1.5 µg/ml polymyxin B; and (E) 0.4 µg/ml gentamicin, 2.0 µg/ml amikacin, 1.0 µg/ml tobramycin, and 3 µg/ml streptomycin, respectively. All experiments were performed in at least three biological replicates and error bars represent mean (± SD. * $p < 0.05$, ** $p < 0.01$, *** $p < 0.001$; student's t test, calculated relative to cultures treated with antibiotics alone).

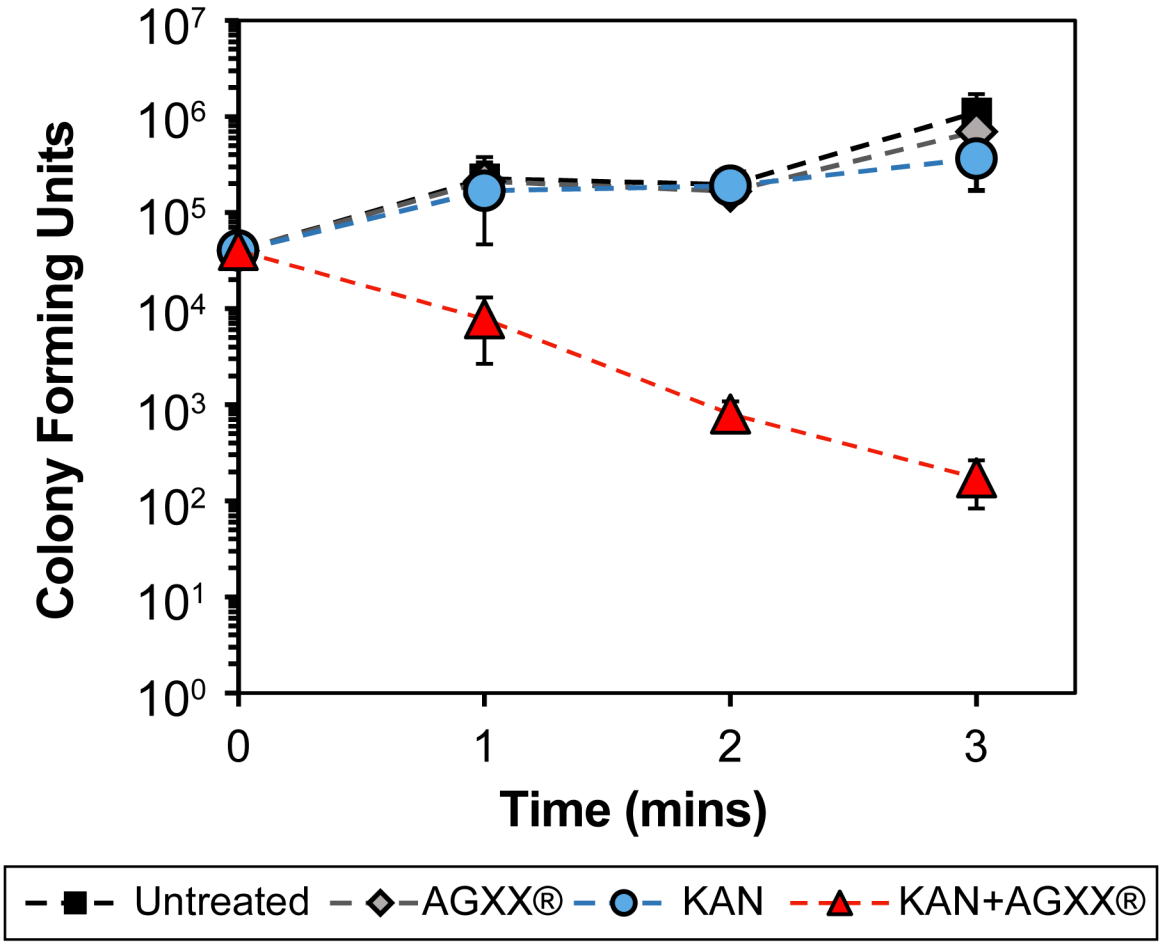

FIG 3 AGXX® increases the sensitivity of *P. aeruginosa* strain PA14 to kanamycin. Overnight PA14 cultures were diluted ~25-fold into Mueller-Hinton media (OD_{600}=0.1) and either left untreated or exposed to 75 µg/ml AGXX720C®, 50 µg/ml kanamycin, or the combination thereof for 3 hours. Samples were taken every 60 minutes, serial diluted and plated on LB agar for CFU counts, (*n=4, ± S.D)*.

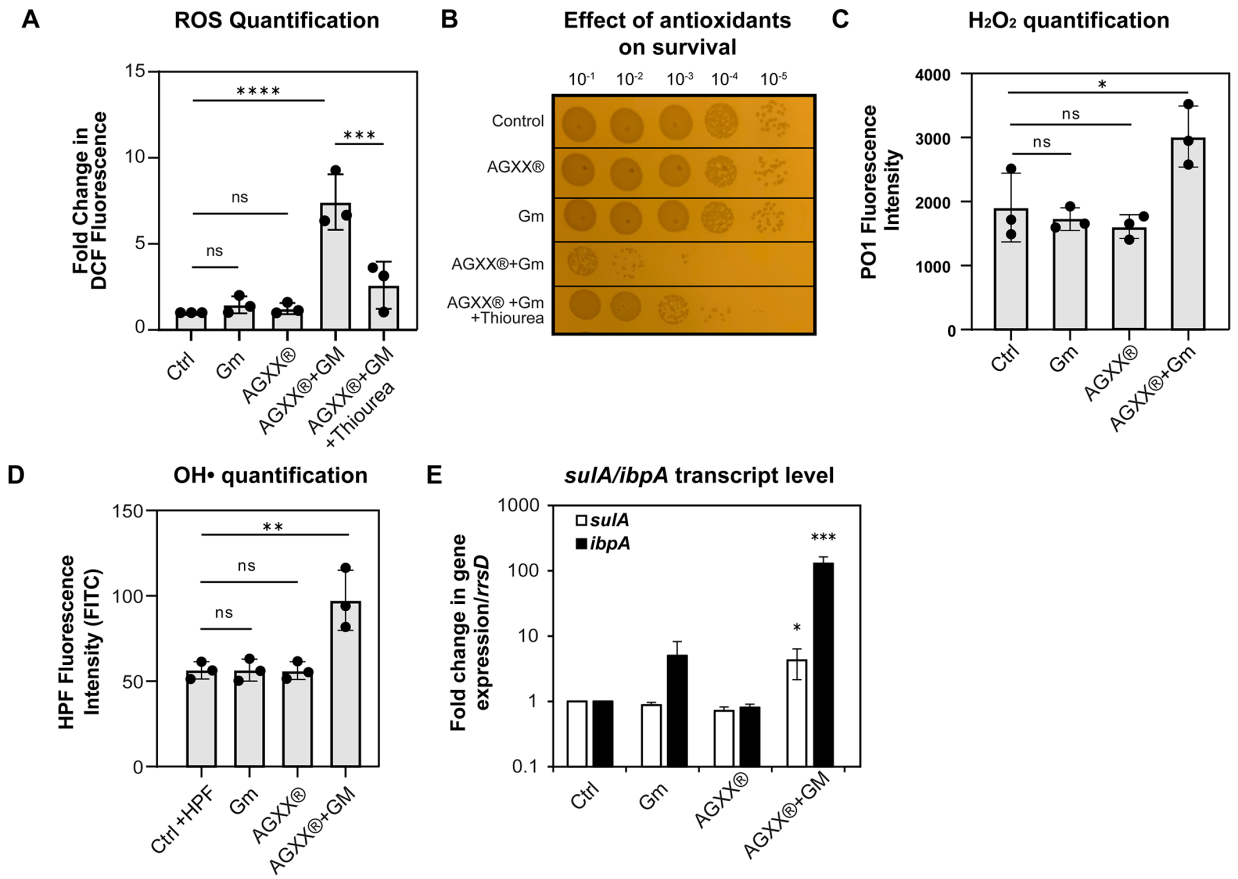

FIG 4 The combination of sublethal concentrations of AGXX® and gentamicin increases ROS levels and causes DNA damage and protein aggregation. Mid-log PA14 cells were treated with sublethal concentrations of Gm (0.25 µg/ml), AGXX720C® (50 µg/ml), the combination thereof, or left untreated. **(A)** Intracellular ROS levels were quantified by H_2DCFDA fluorescence. 50mM thiourea was used as a ROS quencher (*n=3, ± S.D.)*. **(B)** Samples were serially diluted in PBS after 60 min of incubation, spot-titered onto LB agar and incubated for 20 hours. One representative of three independent experiments with similar outcomes. **(C, D)** Cells were strained with **(C)** 10 µM peroxy-orange 1 (PO1) and **(D)** 10µM hydroxyphenyl fluorescein (HPF) for 60 min and fluorescence was measured via flow cytometry (*n=3, ± S.D.)*. **(E)** The induction of *sulA* (white bar) and *ibpA* (black bar) transcript levels was determined by qRT-PCR. Gene expression was normalized to the housekeeping gene *rrsD* and calculated as fold changes based on expression levels in the untreated control (*n=3, ± S.D.*; One-way

ANOVA, Dunnett's posttest; *ns*=*p*>*0.05,* * $p < 0.05$, ** $p < 0.01$, *** $p < 0.001$, **** $p < 0.0001$).

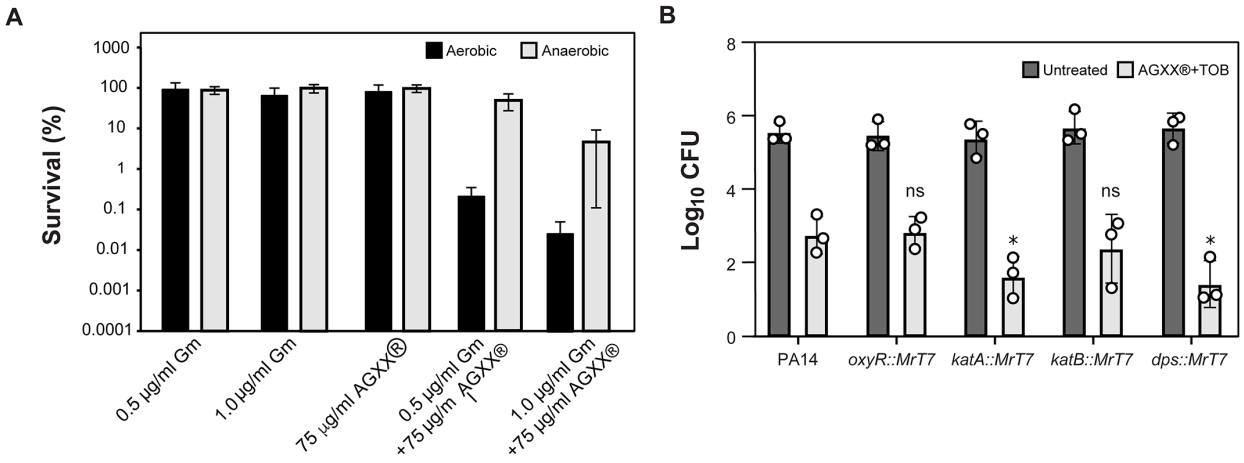

FIG 5 Anaerobic growth and antioxidant systems provide protection against ROS-mediated damage caused by a combinational treatment of AGXX® and aminoglycosides. (A) PA14 were diluted approximately 1000-fold (OD_{600}=0.002) in MHB supplemented with 1% KNO_3 and grown under aerobic (black bars) and anaerobic (grey bars) conditions, respectively. At OD_{600} ~0.2, cultures were treated with either 0.5 µg/ml or 1.0 µg/ml Gm alone or in combination with 75 µg/ml AGXX® for four hours. Cells were subsequently plated onto LB agar for 20 hours at 37°C to enumerate surviving colonies (*n=3,* ± *S.D.*). **(B)** Overnight cultures of PA14 wildtype and mutant strains with MrT7 transposon insertions in *oxyR, katA, katB* and *dps* were diluted into MOPSg to an OD_{600}=0.01 and grown under aerobic conditions until OD_{600}=0.1. Cultures were either left untreated (grey bars) or treated with a combination of 0.25 µg/ml tobramycin and 25 µg/ml AGXX720C® (white bars). Bacterial survival was quantified after two hours by serially diluting cells in PBS and plating on LB agar for 20 hours at 37°C (*n=3,* ± *S.D*; Student t-test, * $p < 0.05$).

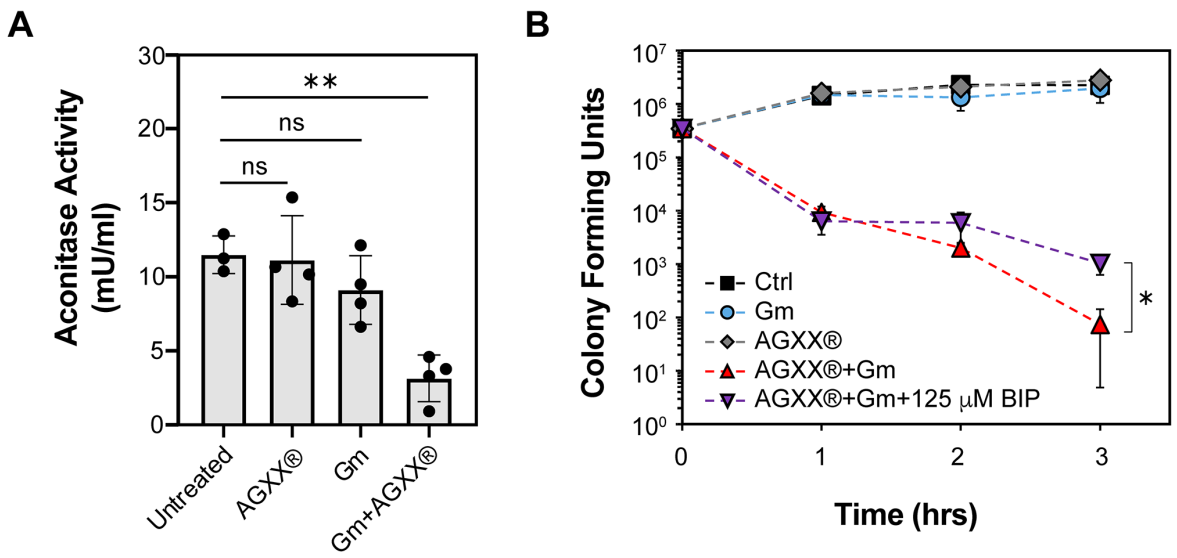

FIG 6 The synergy between AGXX® and aminoglycosides on PA14 killing is in parts mediated by a disruption in iron homeostasis. Overnight PA14 cultures were diluted into MOPSg and incubated under aerobic conditions until exponential phase was reached. **(A)** Cells were left untreated or treated with 100 µg/ml AGXX720C®, 0.6 µg/ml Gm, or the combination thereof for 1 hour. Aconitase activities were determined in crude extracts (*n=4,* ± *S.D*). One-way ANOVA, Dunnett's posttest; *ns p>0.05,* ** $p < 0.01$. **(B)** Cultures were either left untreated (white square) or treated with 0.25 µg/ml Gm (white diamond), 50µg/ml AGXX720C® (white circle), or the combination thereof (white triangle) for three hours. Survival was determined each hour by serially diluting samples in PBS and plating onto LB agar for overnight growth. The impact of free iron on the increased killing by AGXX®/Gm cotreatments was tested by the absence (white triangle) and presence (black diamonds) of 125 µM 2',2' bipyridyl (*n=3,* ± *S.D.*). Student's t test, * $p<0.05$).

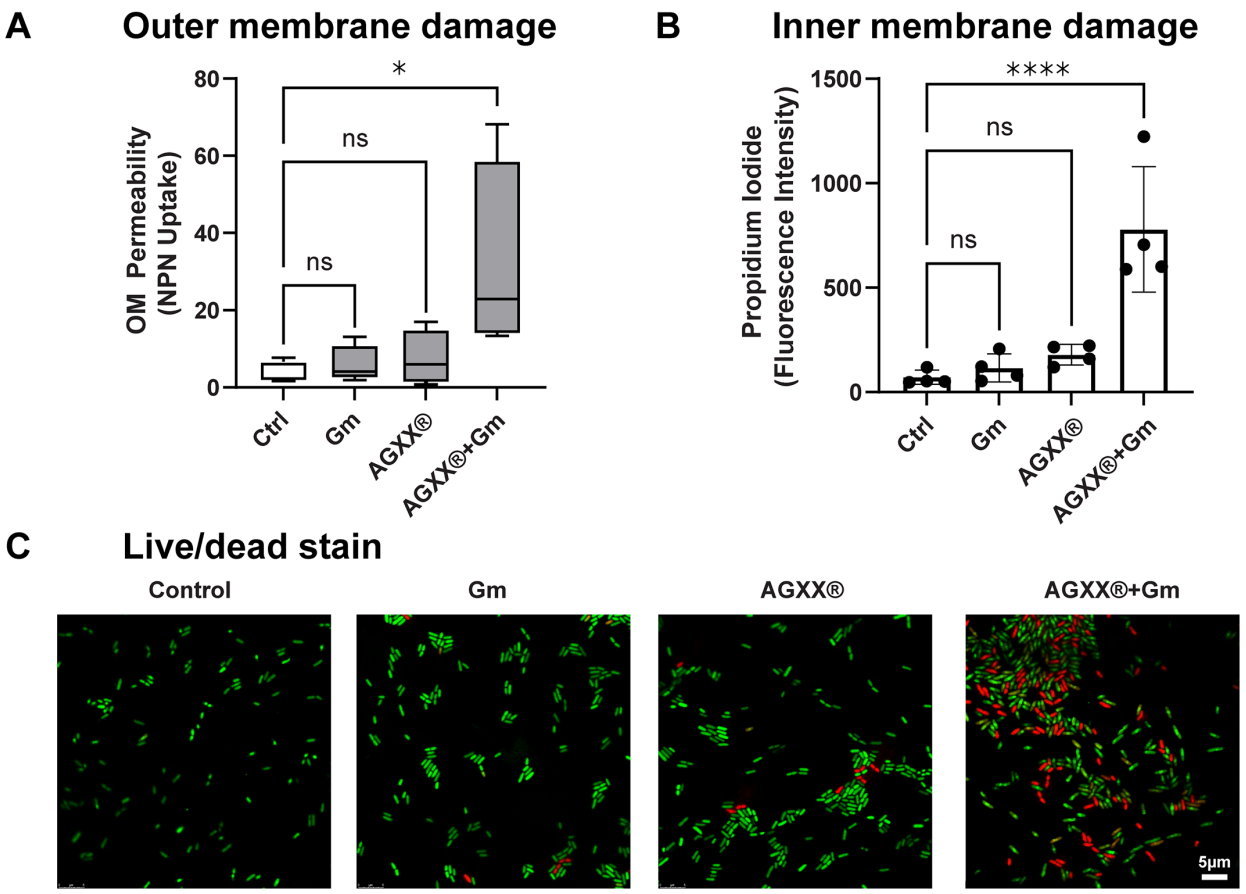

FIG 7 Combined AGXX® and aminoglycoside treatment induces significant membrane damage. PA14 cells grown to mid-log phase in MOPSg media were left untreated or treated with sublethal concentrations of Gm (0.25 µg/ml), AGXX720C® (50 µg/ml), and the combination thereof. Cells were harvested after 1 hour of treatment, washed in PBS, and stained with **(A)** 10 µM N-phenyl-1-naphthylamine (NPN) dye, and **(B)** 0.5 µM propidium iodide (PI). Fluorescence intensities were determined at excitation/emission wavelengths of **(A)** 350/420 nm and **(B)** 535/617 nm, respectively, (*n=4,* ± *S.D.*). One-way ANOVA, Dunnett's posttest; *ns* $p>0.05$, * $p < 0.05$, **** $p < 0.0001$. **(C)** Samples were washed in PBS, stained with PI/Syto9, incubated in the dark for 15 minutes at room temperature, mounted onto a glass slide with 1% agarose, and imaged at 63x magnification via inverted confocal microscopy. One representative of three independent experiments with similar outcomes.

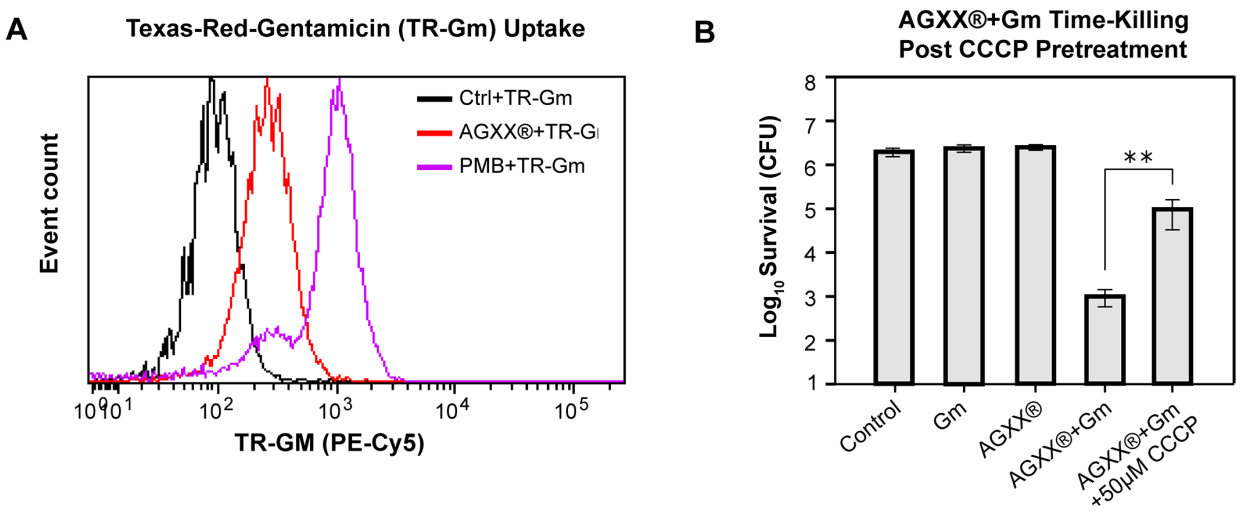

FIG 8 AGXX® increases aminoglycoside uptake and lethality through increased activity of the proton motive force (PMF). (A) Mid-log PA14 cells were treated with 1.0 μg/ml TR-Gm, 1.0 μg/ml TR-Gm + 50 μg/ml AGXX720C®, and 1.0 μg/ml TR-Gm + 2.0 μg/ml polymyxin B (PMB) for 1 hour, respectively. TR-Gm uptake was measured via flow cytometry. **(B)** Mid-log phase PA14 were left untreated (control) or exposed to 0.25 μg/ml Gm, 50 μg/ml AGXX720C® or 0.25 μg/ml Gm + 50 μg/ml AGXX720C® for 3 hours. Samples were serial diluted, plated on LB agar, and incubated for 20 hours for CFU counts. To test the impact of the PMF on the killing of a combination of AGXX® and aminoglycosides, PA14 were pretreated with or without 50 μM carbonyl cyanide *m*-chlorophenyl hydrazone (CCCP) prior to AGXX®/Gm exposure *(n=3, ± S.D.)*. Student's t test, ** $p<0.01$.

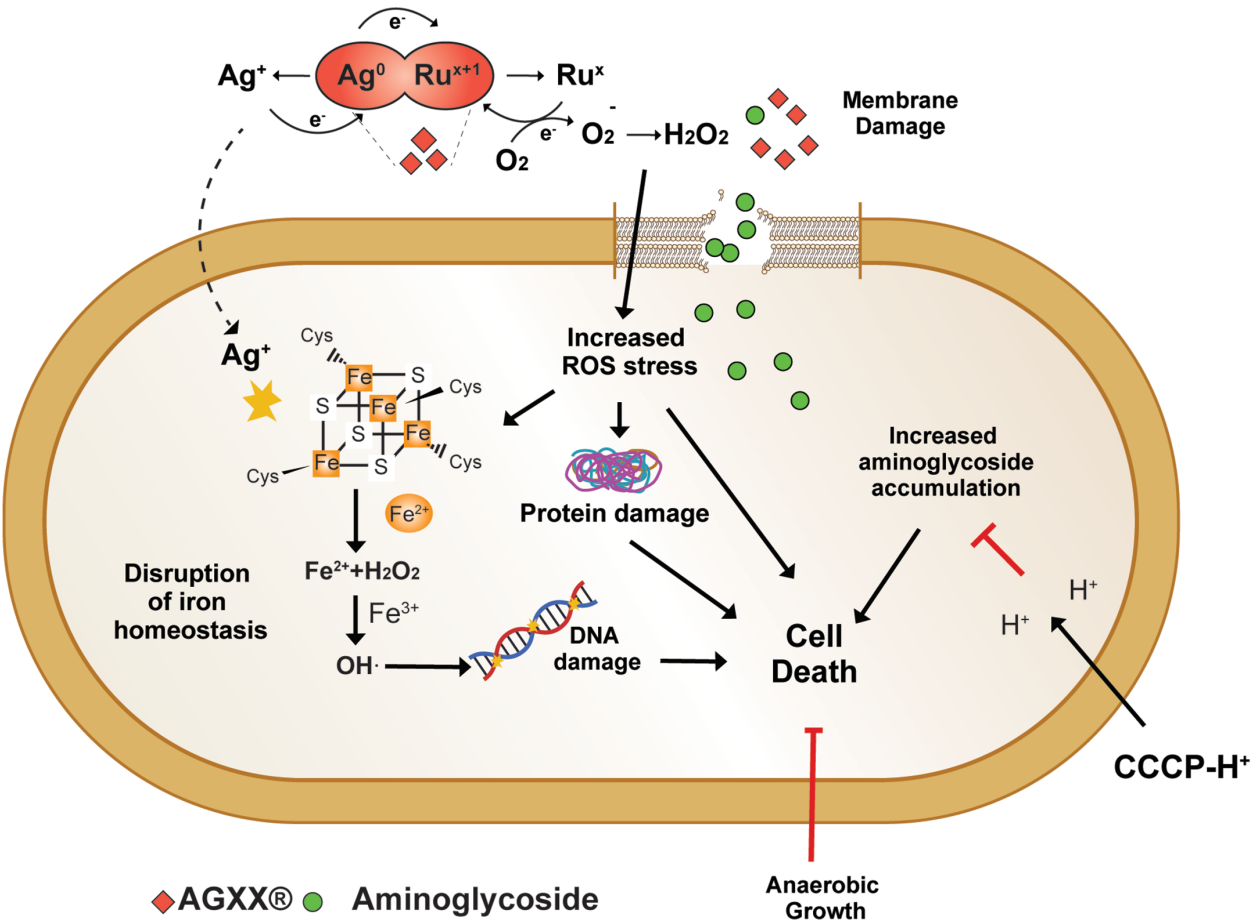

FIG 9 Proposed model for the synergy between AGXX® and aminoglycoside antibiotics. The antimicrobial action of AGXX® is mediated by superoxide (O_2^-) and hydrogen peroxide (H_2O_2), which are generated in a redox cycle between silver (Ag) and ruthenium (Ru^{x+1}). The combination of AGXX® and aminoglycosides concertedly increases endogenous ROS levels. As such anaerobic growth suppressed the synergistic interaction between the two antimicrobials at lower Gm concentrations. Potentially facilitated by a release of silver ions, the increased ROS level may disrupt iron-sulfur clusters in metabolic enzymes such as aconitase, resulting in the release of free iron, which ultimately triggers hydroxyl radical (•OH) formation in a Fenton reaction. Increasing ROS levels can inflict macromolecule damage such as DNA damage and protein aggregation, contributing to increased killing as observed for *P. aeruginosa* that were treated with a combination of AGXX® and aminoglycosides. The synergistic effect

between AGXX® and aminoglycosides is also mediated by an increased uptake and the cellular accumulation of aminoglycosides, which can be attenuated by disrupting the bacterial membrane potential with ionophores such as CCCP.